Master's Thesis

Exploring the Potential of Enzymes to Combat Acne

By Mikaela Fransson and Åsa Leide

Supervisors: Adel Elsayed Attia Abouhmad & Dietlind Adlercreutz

Examiner: Carl Grey

A Collaboration between

ZymIQ Technology AB and Lund University

LUND UNIVERSITY

23 January 2024 – 11 June 2024

Division of Biotechnology

Lund University

Acknowledgement

This master's thesis project has been a collaboration between ZymIQ Technology AB and the Division of Biotechnology at Lund University.

First and foremost, we would like to extend our warmest thanks to our supervisor at ZymIQ, Dietlind Adlercreutz, for her support and valuable knowledge during our master's work. We also want to give special thanks to our supervisor at Lund University, Adel Elsayed Attia Abouhmad, for his guidance throughout this project. The completion of this study would not have been possible without the expertise of Jana Kassaliete, who supervised us through our laboratory work.

We also would like to thank Dr. Carl Grey for accepting the role as examiner.

Finally, we extend our sincerest gratitude to our colleagues at ZymIQ for being so welcoming, with special mention to co-worker Karolina Torfgård and CTO Mats Clarsund.

Abstract

Acne vulgaris is a widespread skin disease affecting approximately 9.4 % of the population. It arises from four primary factors: increased sebum production, hyperkeratinization, bacterial colonization, and inflammation, leading to both non-inflammatory and inflammatory lesions. Current treatments include topical and systemic anti-inflammatory agents, antibiotics, and retinols, which often have adverse effects like dry, irritated skin, and contribute to antibiotic resistance. Therefore, alternative treatments are desirable. *Cutibacterium acnes*, a Gram-positive bacterium involved in the pathogenesis of acne, forms biofilms that hinder treatment efficacy. Enzymes such as proteases, nucleases and lysozymes have shown potential in eradicating these biofilms, thereby preventing the formation of acne lesions without irritating the skin.

In this study, biofilms were grown on 96-well polystyrene plates and exposed to varying concentrations of different enzymes. Crystal violet and resazurin assays were conducted to assess biofilm growth and eradication. Results indicate that nucleases show potential in eradicating biofilms, whereas proteases did not exhibit consistent biofilm-degrading abilities. However, the studies on the enzymes are not conclusive, and dose dependency could not be interpreted. Since the current conditions may have disrupted the biofilm maturation, further studies with a modified experimental design optimized for biofilm growth are required.

Current treatments for acne are limited and often inadequate. Continued research on enzymes could pave the way for viable alternative treatment options for acne patients.

Table of content

Abbreviations

Abbreviation	Meaning
BHI	Brain Heart Infusion
BPO	Benzoyl peroxide
cAMP	Cyclic AMP
CPNP	Cosmetic products notification portal
CRISPR	Clustered regularly interspaced short palindromic repeats
CV	Crystal violet
DNase	Deoxyribonuclease
EPS	Extracellular Polymeric Substances
eDNA	Extracellular DNA
GMP	Good manufacturing practice
GPSD	General product safety directive
GPSR	General product safety regulation
mAbs	Monoclonal antibodies
MDR	Multidrug-resistant
MLST	Multi-locus sequencing
OD	Optical density
PSU	Pilosebaceous unit
PNG	Peptidoglycan
RAPD	Random amplification of polymorphic DNA
RoxP	Radical oxygenase
rRNA	Ribosomal RNA
RT	Ribotype
SG	Sebaceous gland
SLST	Single-locus sequencing type
SSI	Surgical site infection
Tad	Tight adhesion
WGS	Whole genome sequencing

1. Introduction

Acne vulgaris is a widespread skin condition affecting approximately 9.4% of the global population, of which 85% are teenagers and young adults. The disease typically causes significant discomfort, both physical and physiological, due to pain, scarring, and potential disfigurement. [1] Acne arises from four primary factors: increased sebum production, hyperkeratinization of the pilosebaceous unit (PSU), hyperproliferation of *Cutibacterium acnes* (*C. acnes*), and an inflammatory response. Various treatments are available, including topical agents, as well as oral medications. However, these treatments come with drawbacks such as adverse effects, extended regimens and antibiotic resistance. [2]

C. acnes, a Gram-positive, lipophilic, anaerobic bacterium found naturally on the skin, becomes problematic when it proliferates excessively, contributing significantly to acne development by causing lesions such as pustules, papules, and nodules. This overgrowth is facilitated by an overproduction of sebum within the PSU. [2, 3, 4]

In adverse environments, certain strains of *C. acnes* can form biofilms, which exhibit multicellular behavior and produce an extracellular matrix to withstand external stress. These biofilms are composed of extracellular polymeric substances (EPS), including polysaccharides, proteins, and extracellular DNA (eDNA). Biofilm formation can make bacteria up to 1000 times more resistant to antibiotics than planktonic cells, necessitating alternative therapeutic strategies. [5]

Antibiotics are considered as a leading solution in current healthcare, but the rise of resistant bacteria poses a significant threat to modern medicine, with approximately 700,000 deaths from infections caused by multidrug-resistant (MDR) bacteria annually, a number estimated to reach 10 million by 2050. [1]

The escalating problem of antibiotic resistance has spurred research into alternative approaches for combating bacterial infections. One promising alternative is antibacterial enzymes (Enzybiotics) that target the bacterial cell wall.

In acne, some enzymes are thought to counteract hyperkeratinization, while others have matrix-degrading properties and may counteract biofilm formation or disintegrate the biofilm. [6] Additionally, other enzymes target the cell walls of Gram-positive bacteria and are potentially promising in the therapeutic combat of acne. [7]

1.1 Aim

The aim of this project is to examine the potential of using enzymes to target the biofilms of *C. acnes* in the treatment of acne. Through literature studies, we aim to gain deeper understanding of the factors causing acne and investigate how current treatments can be replaced to minimize adverse effects. Enzymes such as proteases, nucleases, and lysozymes will be tested in vitro against *C. acnes* to assess their effectiveness in degrading biofilm and reducing bacterial counts.

2. Background

2.1 Acne vulgaris

2.1.1 Occurrence

The high rates of individuals affected by acne vulgaris [8] makes it the eight most common skin disease in the world. The etiology of acne vulgaris involves various factors that could contribute to its onset, progression, and aggravation. These factors include genetics, environmental variables like temperature, humidity and sun exposure, dietary habits, hormonal fluctuations, and stress levels. Furthermore, smoking, the use of comedogenic medications such as androgens and corticosteroids, bacterial presence, and the use of cosmetics are also contributing factors. [1]

Acne often emerges during puberty, likely due to hormonal imbalances and increased stress levels. Acne vulgaris can be physically painful, particularly in cases with significant inflammation, and it can also be emotionally distressing. The visible effects of acne outbreaks and the potential for permanent scarring can lead to anxiety, embarrassment, and even depression. [1, 9]

2.1.1.1 The pilosebaceous unit

The pilosebaceous unit, an essential structure of the skin, includes the hair follicle, sebaceous gland (SG), and arrector pili muscle, as shown in Figure 1. These units are distributed all over the body, except on the palms and soles, with higher density on the face, neck, chest, and upper back. The “T-zone” - forehead, nose, and chin – features the densest population of sebum-secreting SGs. Although the SGs on the face are larger, they have smaller sebaceous ducts,

creating greater resistance to sebum output compared to other areas. This resistance is a key factor in pilosebaceous skin diseases such as acne. [9, 10, 11]

Sebum, produced by the SGs, consists of triglycerides, free fatty acids, wax esters, squalene, and cholesterol. It is essential for maintaining skin homeostasis. Androgen hormones, particularly during puberty, stimulate sebum secretion, contributing to changes in skin condition. [12]

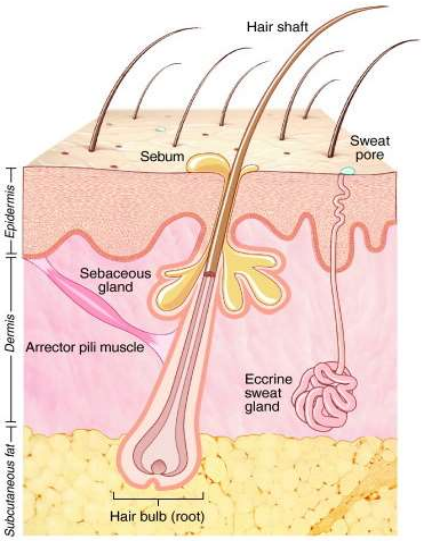

Figure 1. A human skin illustration showing the hair follicle, SG where sebum is produced and excreted, hair shaft, arrector pili muscle, sweat gland, and the three layers of the skin that the PSU traverses. [13]

2.1.2 Pathogenesis

Several factors contribute to acne, including excess sebum production, follicular hyperkeratinization, hyperproliferation of *C. acnes,* and inflammation. These factors are interconnected, leading to the formation of papules, pustules, and comedones, as shown in Figure 2. The pilosebaceous unit is colonized by both healthy and pathogenic strains of *C. acnes*. Increased hormone levels boost sebum production, and together with hyperkeratinization, clog the pore, creating a more anaerobic environment within the SG. This environment favors acneic *C. acnes* strains, which release tissue-degrading enzymes and other virulence factors. These changes promote closer contact with keratinocytes and sebocytes, triggering a local immune response and resulting in inflammatory acne. [14]

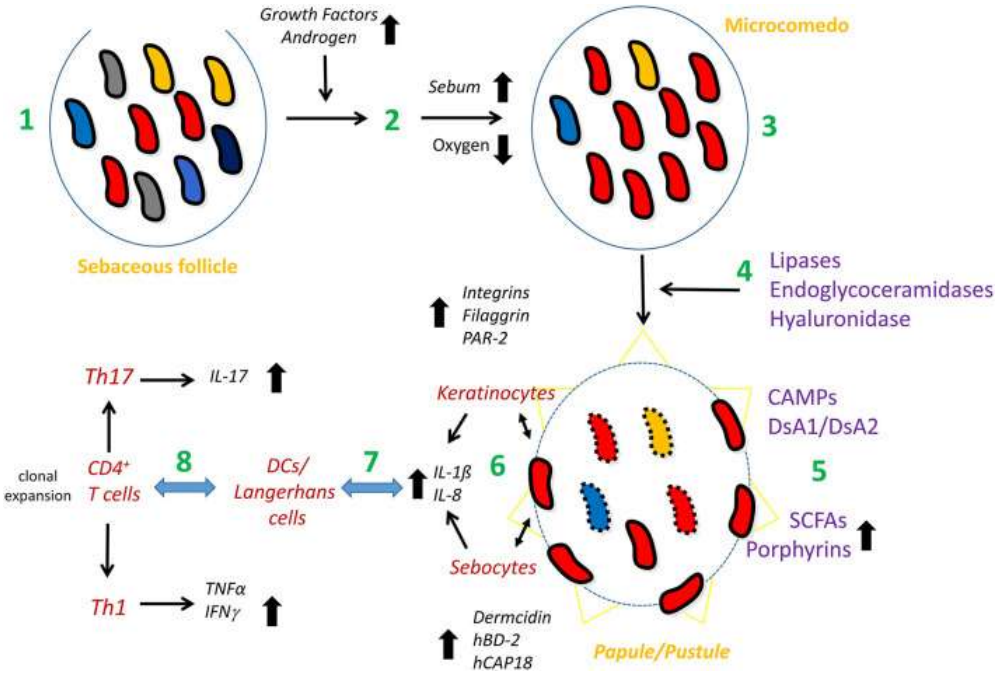

Figure 2. Model of *C. acnes* involvement in acne vulgaris. [14]

2.1.2.1 Increased sebum production

One primary cause of acne is the overproduction of sebum in hair follicles. This increase in sebum synthesis and secretion is believed to be influenced by androgen hormones such as testosterone. The severity and frequency of acne lesions strongly correlate to the amount of sebum produced. [1]

2.1.2.2 Follicular hyperkeratinization

The second stage of acne pathogenesis involves hyperkeratinization within hair follicles and SGs, playing a pivotal role in lesion development. Hyperkeratinization is a process in which follicular epithelial cells exhibit abnormal proliferation and shedding behavior. It inhibits the proper release of keratinocytes into the lumen, leading to the accumulation of sebum and a decrease in oxygen levels inside the clogged follicle. This initiates the formation of a microcomedon under the skin, gradually progressing into a more prominent and visible comedo. [1, 15]

2.1.2.3 Hyperproliferation of *C. acnes*

C. acnes is anaerobic bacteria that thrives in the oxygen-deprived environment of clogged PSUs, with the overproduction of sebum providing a rich nutrient source for its growth. It metabolizes sebum triglycerides into fatty acids and glycerol using lipase enzymes, triggering inflammation of the comedones on the skin. [1] Different strains of *C. acnes* are associated

with varying degrees of acne severity due to their release of different virulence factors and their potential to form biofilms. Understanding the distinction between acneic and non-acneic strains is crucial for developing targeted treatments. The different strains are discussed further in section 2.2.2.

2.1.2.4 Inflammation

Upon detection by the immune system, *C. acnes* in contact with keratinocytes and sebocytes initiates an innate immune response, leading to the recruitment of lymphocytes, macrophages, and neutrophiles to the site of infection. This is followed by the release of cytokines such as IL-8 and IL-1β. The irritated tissue is infiltrated by recruited skin-resident macrophages and DCs/Langerhans cells. They also interact with skin-resident CD4+ T cells, leading to clonal expansion and differentiation into Th1 and Th17 cells. Responses from Th1/Th17 cause the secretion of other cytokines such as IFN-γ and IL-17. These inflammatory cascades within the follicle form lesions such as pustules, nodules, cysts, or papules on the skin. [1, 14]

2.1.3 Types of skin lesions

Acne vulgaris presents with a variety of skin lesions, typically comprising both non-inflammatory open and closed comedones, as well as inflammatory papules, pustules, nodules, and cysts. Each type exhibits a distinct appearance on the skin, as depicted in Figure 3. [16]

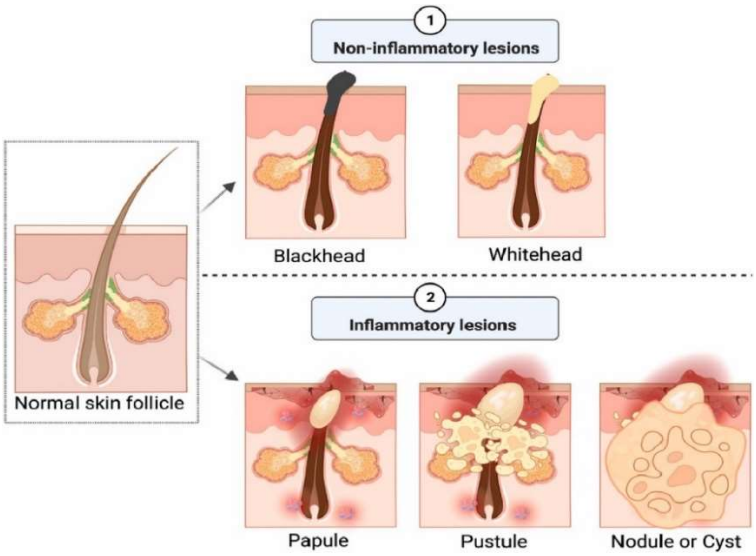

Figure 3. An illustration of the healthy hair follicle, as well as the non-inflammatory and inflammatory lesions. [1]

2.1.3.1 Non-inflammatory lesions

The mildest forms of acne lesions are non-inflammatory open and closed comedones. Open comedones, often referred to as blackheads, develop when excess oils and dead skin cells block the hair follicle opening, resulting in dark dots on the skin surface. Upon exposure to oxygen, the debris oxidizes, causing a color change. [17] Closed comedones, or whiteheads, form from excess sebum, bacteria, and skin cells obstructing the hair follicle pores, leading to small white bumps on the skin surface. While both blackheads and whiteheads follow similar disease progressions, they manifest differently on the skin. [1, 16]

2.1.3.2 Inflammatory lesions

More severe forms of acne lesions include inflammatory papules, pustules, nodules, and cysts, which are major contributors to acne-related skin issues due to their often-prominent visibility and associated pain. Papules represent an intermediate stage between non-inflammatory and inflammatory lesions, where an inflammatory response is triggered by the release of keratinocytes and sebocytes in the pathogenesis cascade [14], leading to redness and swelling. These lesions, a consequence of bacterial presence, excess sebum production, and increased androgen activity, appear as smaller pink bumps on the skin. Subsequent stages involve pustules, typically presenting as white pimples filled with pus and surrounded by redness. [1, 16]

Nodules signify a more severe form of acne, resembling papules but larger, emerging when pores are obstructed by bacteria, excess sebum, and dead skin cells. The infection penetrates deeper into the skin and inflammation is triggered. The ultimate stage of acne lesions is cystic acne, caused by blocked hair follicles where inflammation extends further into the skin. These lesions appear as larger, red and white bumps on the skin, filled with pus. [1, 16]

2.1.4 Current Treatments

Numerous treatments are currently available for acne vulgaris, aiming to address its underlying causes such as excessive sebum secretion, abnormal hyperkeratinization, and bacterial infection. These treatments target existing lesions through antibacterial or anti-inflammatory mechanisms and can be administered topically, orally, or systemically. [1]

2.1.4.1 Topical Treatments

Antibiotics

Mild to moderate inflammatory acne is commonly treated with topical antibiotics like **clindamycin** and **erythromycin**. These antibiotics act in the PSUs to reduce *C. acnes* colonization and inflammation. However, erythromycin has shown a 60% increase in antibiotic resistance, prompting the exploration of alternative topical antibiotics. [1]

Combinational topical treatments

To mitigate antibiotic resistance, topical antibiotics are often combined with benzoyl peroxide (BPO) and topical retinoids. This combinational therapy addresses various factors contributing to acne development. Common topical treatments include BPO, salicylic acid, and niacinamide. **BPO** has antibacterial properties and acts as a disinfectant through the release of oxygen radicals. The beta hydroxy compound **salicylic acid** has both anti-inflammatory and bacteriostatic properties**,** aiding in skin exfoliation and pore clearance, thereby reducing acne occurrence. While salicylic acid may cause skin irritation, it is generally safe to use. **Niacinamide,** also known as nicotinamide, is a form of vitamin B3 that reduces sebum secretion, shielding the skin from acne development. [1, 6]

Retinoids

Retinoids, vitamin A derivatives, are a first-line treatment for acne aimed at reducing sebum production, regulating comedone growth, and preventing new lesion formation. Although effective, retinoids can be time-consuming and cause skin irritation and dryness. Commonly used retinoids include tretinoin, adapalene, and tazarotene. **Tretinoin** has anti-inflammatory properties and is often combined with other retinoids to normalize the epithelial layer and reduce sebum production. **Adapalene** is considered a first-line therapy due to its advantages, including minimal skin side effects while reducing inflammation and hyperkeratinization. **Tazarotene** serves as a second-line acne treatment used when adapalene and tretinoin are ineffective, helping to reduce hyperkeratinization and hyperproliferation of *C. acnes* [1]

2.1.4.2 Systemic treatments

When first-line topical retinoids fail or lesions appear as nodules or cause scars, oral systemic treatments are considered. The most common systemic treatments are antibiotics, hormonal medications, and the retinoid isotretinoin.

Antibiotics

Oral antibiotics are prescribed for moderate to severe inflammatory acne or extensive lesions. Tetracyclines, clindamycin, and azithromycin suppress *C. acnes* growth and reduce inflammation. However, these broad-spectrum antibiotics affect the entire skin microbiota, suppressing beneficial bacteria. Due to the risk of bacterial resistance, antibiotics are administered in small doses over extended periods and are often combined with topical agents like benzoyl peroxide or retinoids to improve efficacy and minimize resistance development. [1, 18]

Retinoids

Isotretinoin, a systematic retinoid and vitamin A derivative, is a first-line treatment for severe acne, targeting all four virulence factors of acne. It decreases sebum production, alters the cutaneous bacterial flora, diminishes *C. acnes* colonization, and aids in keratinocyte shedding in follicles. Despite its effectiveness, the treatment lasts 16-24 weeks and it requires careful monitoring due to adverse effects like transient peeling, scaling, dryness, and skin irritation. The treatment can also exacerbate hyperpigmented lesions due to inflammatory responses, which vary by skin type. [18, 19]

Hormonal treatment

Hormone therapy, typically in the form of oral contraceptives, is valuable for adolescent and adult females with acne. These contraceptives reduce sebum production by inhibiting androgen induction and increasing globulin synthesis, thereby reducing active free testosterone. Hormonal contraceptives can be used alone or with complementary therapies. However, to achieve noticeable effect, the treatment period spans a minimum of 12 months. [18]

2.2 *Cutibacterium acnes*

Cutibacterium acnes is a part of the skin microbiota, commonly found in regions abundant in PSUs where it thrives in the oily environment created by the sebum produced by the SGs. While considered a commensal bacterium, its involvement in skin conditions such as acne vulgaris also classifies it as an opportunistic pathogen. [9]

2.2.1 Taxonomy / Classification

Cutibacterium acnes, formerly known as *Propionibacterium acnes*, belong to the phylum *Actinobacteria*. The re-classification aimed to better align with the bacterium's function and characteristics. [9] Within the genus *Cutibacterium*, *C. acnes* was further divided into three subspecies, based on gene expression or lipase activity, which are *C. acnes* subsp. *acnes* (phylotype I), *C. acnes* subsp. *defendens* (phylotype II) and *C. acnes* subsp. *elongatum* (phylotype III). [9, 20]

2.2.2 Strains

Various analytical techniques, including random amplification of polymorphic DNA (RAPD) analysis, sequencing of genes like *RecA* and *tly*, and the use of specific monoclonal antibodies (mAbs), facilitate the discrimination of *C. acnes* strains by further identifying genetic and phenotypic variations. By using these analysis methods, *C. acnes* subspecies could be classified into phylotypes I, II, and III based on characteristics such as cell wall composition, sugar contents, and morphology. Additional methods, such as multi-locus sequence typing (MLST), single-locus sequence typing (SLST), and whole genome sequencing (WGS), allowed for strains to be further categorized into clades based on genetic differences. The MLST method based on first nine, then eight housekeeping genes (MLST9) further categorizes *C. acnes* strains into six phylotypes: IA_1, IA_2, IB, IC, II and III. [9, 21, 22]

Another method for characterizing *C. acnes* strains is by studying their 16S ribosomal RNA (rRNA) sequences. Through 16S rRNA gene ribotyping, ten major ribotypes (RTs) can be identified, with ribotype 1 (RT1) being the most abundant, followed by RT2, and so forth. These RTs exhibit some variations in their genome sequences, which may influence their involvement in acne vulgaris. However, ribotype classification has limitations due to shared RTs across clades. [22, 23] The SLST method, similar to MLST but capable of comparing multiple strains within a complex microbial environment, further classifies *C. acnes* strains into 41 distinct SLST types. [22]

These DNA-based techniques are collectively used to gain a comprehensive understanding of the complex *C. acnes* strains, and to effectively characterize the main phylotypes, all presented in Table 1. Each typing method has its own limitations and benefits, underscoring the value of employing a combined approach. [22]

Table 1. The characterization of *C. acnes* strains based on DNA-based techniques such as MLST, WGS, and SLST. [22] Additionally, examples of strains are provided. [24]

Subspecies	MLST8	RT (WGS)	SLST	Strain isolates
C. acnes acnes	IA_1	RT1	B1	K107 (JCM18916)
		RT4	C1-5	
		RT5	A1-34	
			D1-D5	
		RT8	E1-9	
	IA_2	RT3	F1-14	K115 (JCM18918)
	IB	RT1	H1-8	K115 (JCM18918)
	IC	RT5	G1	/
C. acnes defendens	II	RT2, RT6	K1-25	K127 (JCM18920)
C. acnes elongatum	III	RT9	L1-10	K57 (JCM18909)

2.2.2.1 *C. acnes* strain involvement in acne vulgaris

Various *C. acnes* strains exhibit pathogenicity through mechanisms like biofilm formation and virulence factor expression that can facilitate cell adhesion, provoke inflammation, induce tissue degradation, and stimulate the synthesis of polysaccharides. Molecular analyses on surface structures of *C. acnes* reveal that phylotype IB and II are prevalent in healthy skin, while phylotype IA predominates in acne patients. [9]

A study made by Fitz-Gibbon and colleagues [23] on *C. acnes* strains in the human skin microbiome showed associations specific to both diseased and healthy skin states. The study found that RT1-RT3 are equally abundant in healthy individuals and acne patients. RT4, RT5, RT7, RT8, RT9, and RT10 were more prevalent in acne patients, while RT6, phylotype II, were strongly associated with healthy skin. Further genome analysis showed that RT4 and RT5, both belonging to phylotype IA_2, are the ribotypes most strongly linked to acne. They carry a plasmid encoding for tight adhesion (Tad) and unique genes linked to increased virulence in host organisms. RT2 and RT6 encode clustered regularly interspaced short palindromic repeats (CRISPR), potentially providing protection against viruses and inflammation. [23, 25]

As illustrated in Table 2, RT4 and RT5 are the main strains associated with acne, rarely found in healthy skin. RT6 has shown a 99% association with healthy skin, and other ribotypes show either unclear results or are evenly distributed between acne patients and healthy individuals. [23, 26]

Table 2. The ten major *C. acnes* RTs and their presence in acneic or non-acneic skin, based on a study made in 2013. [23]

Ribotype	Number of subjects	Number of clones	Percentage of clones from acne patients	Percentage of clones from healthy individuals
RT1	90	5536	48%	52%
RT2	48	1213	51%	49%
RT3	60	2104	40%	60%
RT4	23	275	84%	16%
RT5	15	205	99%	1%
RT6	11	262	1%	99%
RT7	10	188	99%	1%
RT8	5	239	100%	0%
RT9	4	68	99%	1%
RT10	5	61	100%	0%

2.2.3 Characteristics

C. acnes have a rod-shaped morphology, measuring 0.4 to 0.7 µm in width and approximately 3 to 5 µm in length. *C. acnes* thrive in oxygen-deprived environments but can adapt to aerobic conditions through the production of the antioxidant protein radicaloxygenase (RoxP). This enzymatic system allows it to be classified as an aerotolerant anaerobe. [9, 27]

The cell wall composition of *C. acnes* differs from other Gram-positive bacteria; it contains unique elements such as phosphatidylinositol, triacylglycerol and other common lipids. [9] *C. acne*s genome, comprised of around 2,56 million base pairs, features genes for metabolic enzymes for survival in the presence of oxygen and lipases for nutrient acquisition. Virulence factors such as sialidases and adhesins are also found in the genome, genes that are implicated in inflammation and tissue degradation in the host. [9, 28]

2.3 Biofilm formation

To enhance survival in adverse environments, bacteria form biofilms, exhibiting multicellular behavior that increases their resistance to external stress. In response to environmental changes, planktonic cells adhere to surfaces and organize into microcolonies. These microcolonies then evolve into biofilms through further cell division, forming a complex regulatory network (Figure 4). Bacteria produce an extracellular matrix, which constitutes a significant portion of the biofilm's biomass. Biofilm formation not only optimizes nutrient utilization through

synergistic interactions but also alters the expression of surface molecules, endowing the bacteria with properties crucial for survival under harsh conditions. Biofilms can make bacteria up to 1,000 times more resistant to antibiotics compared to planktonic cells. [5] Research has confirmed that several strains of *C. acnes,* including the acneic strains RT4 and RT5, can form biofilms. Furthermore, these biofilm structures are more frequently observed in the follicles of acne patients than in healthy follicles. [2]

2.3.1 Matrix characteristics

Several in vitro studies have explored the composition of the *C. acnes* biofilm matrix, demonstrating that the EPS consists primarily of polysaccharides, eDNA, and proteins (Figure 4). Polysaccharides, especially those with residues of α-mannopyranosyl and α-glucopyranosyl, are predominant in biofilms from skin isolates. For the *C. acnes* RT5 strain, polysaccharides represent 62.6% of the biofilm matrix, proteins 9.6%, and eDNA 4.0%, with the remaining 23.8% consisting of other compounds, including porphyrin precursors. The matrix polysaccharides share similarities with the cell wall of *C. acnes,* containing N-acetylgalactosamine, N-acetylmannosamine, 2-acetamido-2-deoxy-galactose, and 2,3-di-acetamido-2,3-dideoxy-mannuronic acid residues. [2]

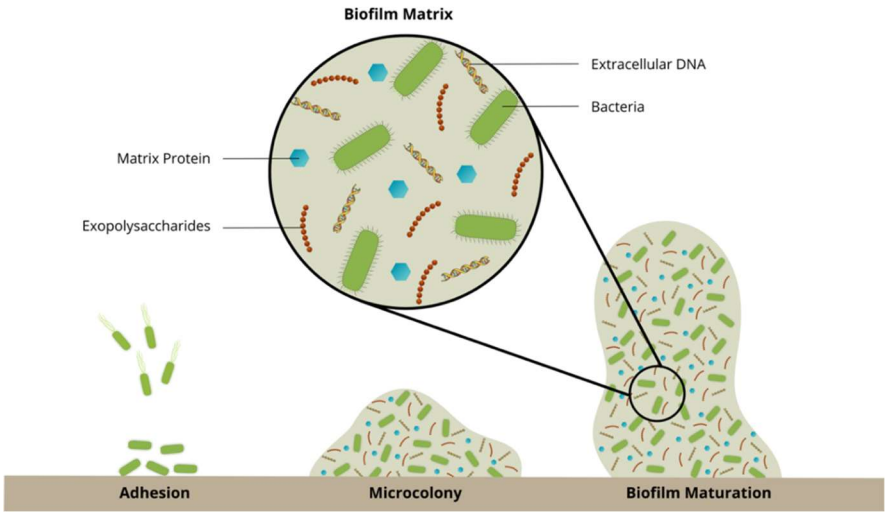

Figure 4. Formation and composition of a general biofilm.

The major polysaccharide in the matrix has the chemical structure →6)-α-D-Galp-(1→4)-β-D-ManpNAc3NAcA-(1→6)-α-D-Glcp-(1→4)-β-D-ManpNAc3NAcA-(1→3)-β-GalpNAc-(1→. These polysaccharides in the EPS facilitate colonization on biotic and abiotic surfaces, promote bacterial aggregation, and provide mechanical stability. This hydrated polymer network supports resistance to host defenses during infection and serves as a nutrient source. [29]

Proteins in the biofilm matrix contribute to adherence to surfaces and interact with exopolysaccharides and nucleic acids, stabilizing the biofilm structure. In the *C. acnes* biofilm, the most abundant of the 447 detected proteins include the chaperonin GroL, elongation factors EF-Tu and EF-G, various glycolytic enzymes, and proteins of unknown function. These matrix proteins aid in attachment and colonization through interactions with cell surface proteins, pili, and flagella. [30, 31]

eDNA, comprised of biopolymers of nucleic acids, provides structural integrity and stabilizes the biofilm matrix, facilitating adhesion, horizontal gene transfer, antibiotic resistance, and protection against host immune responses. It is critical in the initial phases of biofilm formation, aiding bacterial attachment and aggregation on surfaces. eDNA is typically produced by the release of bacterial genomic material into the biofilm matrix through cell lysis. [32]

2.3.2 *C. acnes* biofilms and failure of antimicrobial therapy

The widespread use of antibiotics to treat severe acne has led to the development of antibiotic-resistant *C. acnes* strains, particularly against erythromycin and clindamycin. Over 50% of patients treated with these antibiotics exhibit resistance, and more than 20% have strains resistant to tetracycline. [2] This rising resistance has sparked global concerns, reducing the efficacy of antibiotics in acne treatment. [33]

Biofilm formation by *C. acnes* significantly contributes to the failure of antimicrobial therapies. *C. acnes* biofilms require higher antibiotic doses and longer treatment durations to be effectively disrupted compared to planktonic bacteria. [2]

2.3.3 Assessment for quantifying biofilm formation

The crystal violet (CV) staining assay and the resazurin cell viability assay are two methods used for biofilm characterization. The CV assay monitor biofilm formation directly while resazurin measures viable cells, indirectly corresponding to the amount of biomass. The assays can thereby assess the impact of enzymes on established biofilms. The expected appearance of the resazurin and CV plates after the experiment with varying enzyme concentrations is shown in Figure 5.

For the CV assay on effective enzymes, the color should range from light blue/purple, where the enzyme concentration is high (resulting in a lower absorbance due to greater biofilm breakdown), to darker blue at lower enzyme concentrations (higher absorbance).

The resazurin assay indicates cell viability by color change. For an effective enzyme, high concentrations, correlating with low cell viability, are shown in blue. Conversely, lower enzyme concentrations, which correlate with a higher cell viability, are shown in pink.

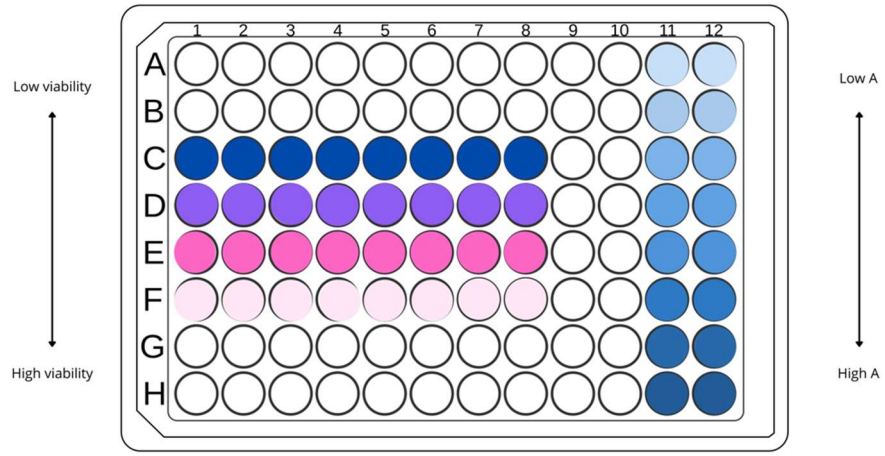

Figure 5. The expected results from the resazurin and CV assays, provided that the enzymes are effective, Enzyme concentrations decrease from high at the top to low at the bottom. Columns 1-8, rows C-F, illustrate the resazurin staining, Columns 11-12 illustrate the CV staining. A = Absorbance

2.3.4.1 Crystal violet assay

The crystal violet assay quantifies biofilm biomass by staining polysaccharides and negatively charged surface molecules within the extracellular matrix of the biofilm. CV staining effectively measures biomass but does not differentiate between metabolically active and inactive cells. [34] Crystal violet is a basic trianiline dye that permeates cell membranes, and absorbance measurements of CV can be performed by first releasing the bound dye with a solvent. This quantification is made using a spectrophotometer and determines the presence and extent of biofilm. [35]

Absorbance measurements are performed by passing light at a specific wavelength through a sample to quantify the dye concentration released from the stained biofilm. Higher absorbance values indicate a higher concentration of cells or biofilm, as more light is absorbed by the dye. [36]

2.3.4.2 Resazurin cell viability assay

The resazurin assay evaluates the viability of living cells within a biofilm. This assay is widely used due to its cost-effectiveness, simplicity, and non-toxic nature to cells. [37] The principle behind the resazurin assay lies in the metabolic activity of living cells, which reduce resazurin, a blue dye, to resorufin, as illustrated in Figure 6. Resazurin exhibits minimal fluorescence,

whereas its reduced form, resorufin, appears pink and is strongly fluorescent. The fluorescence emitted is directly proportional to the number of metabolic active cells present in the sample.

Cell viability measurements are typically performed using a microtiter plate reader, measuring fluorescence intensity with excitation set to 560 nm and emission to 590 nm. [34, 38] Additionally, absorbance measurements can be made at wavelengths of 600 nm and 570 nm for resazurin and resorufin, respectively, providing an alternative method to assess cell viability based on changes in absorbance.

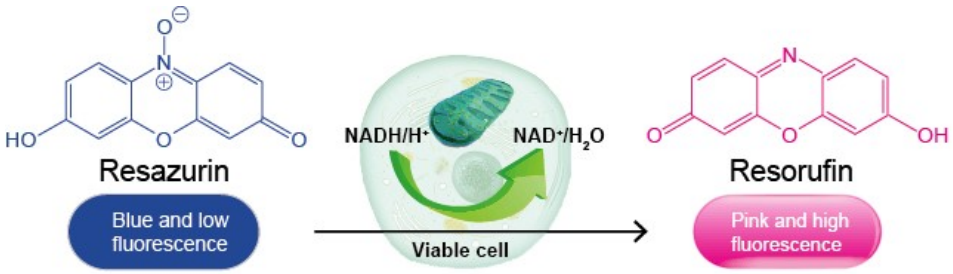

Figure 61. Illustration of the principle of resazurin cell viability assay. [39]

However, the resazurin assay has limitations, especially with large cell populations or prolonged assay durations. While the reduction of resazurin to resorufin is irreversible, a secondary reversible reduction reaction can produce a colorless and non-fluorescent byproduct known as hydroresorufin. This secondary reaction may lead to an underestimation of the actual number of living cells within the sample. [37]

2.4 *Cutibacterium avidum*

Another member of the *Cutibacterium* genus is *Cutibacterium avidum*. *C. avidum* is a commensal bacterium found in the human skin microbiota. Unlike *C. acnes*, it is rarely associated with acne vulgaris, but rather with serious spontaneous and surgical site infections (SSIs). *C. avidum* is an anaerobic-aerotolerant Gram-positive rod-shaped bacterium present on the skin surfaces of both healthy individuals and acne patients. While *C. acnes* predominantly resides in regions with SGs, *C. avidum* is mainly colonized in moist areas with sweat glands, such as the nares, axilla, and groin. Further studies on *C. avidum* strains are essential to elucidate its ability to adhere to surfaces, form biofilms, and its interactions with the immune response. Similar to other *Cutibacterium* species, *C. avidum* exhibits high susceptibility to various antimicrobial therapies. [40, 41]

2.5 Enzymes for acne treatment

Today, enzymes are not commonly used for acne treatment, but various enzyme-based treatment options have been suggested in scientific literature. Historically, chemicals have been used to remove or inhibit biofilms; however, their toxicity and environmental risks have led to the exploration of enzymes as safer alternatives in medical applications. Acne is a multifactorial disease characterized by excess sebum production, follicular hyperkeratinization, hyperproliferation of *C. acnes*, and inflammation, with the latter two factors closely associated with *C. acnes* biofilm formation. [7, 42]

Enzymes can address several factors contributing to acne, providing a milder alternative to many current treatments. Proteases, nucleases, and glycosidases can break down biofilm matrix components, making planktonic cells more susceptible to host immune responses and antimicrobials. Biofilm matrix-degrading enzymes thus represent a promising alternative to antibiotics and anti-inflammatory drugs. [7, 42]

Other enzymes, such as lysozymes, offer an alternative to antimicrobials by breaking down bacterial cell walls. Lysins, enzymes derived from phages, can selectively lyse specific bacteria, leaving the healthy microbiome intact. [7, 42]

2.5.1 Proteases

Proteases, enzymes adept at cleaving peptide bonds, play a key role in disrupting biofilm matrices. Their action has demonstrated effectiveness both in inhibiting biofilm formation and in dispersing established biofilms. Within the biofilm matrix, exoproteins are integral to bacterial cell aggregation, surface adhesion, and overall structural integrity. By degrading these exoproteins with the enzymatic action of proteases, biofilm eradication becomes more efficient. [7, 43]

Furthermore, proteases exhibit exfoliating properties by altering proteins in the epidermis and dermis, facilitating the removal of damaged skin. This process holds particular significance in addressing conditions like acne vulgaris, characterized by hyperkeratinization leading to the accumulation of dead skin cells within the PSU. Protease-mediated exfoliation targets skin proteins such as keratin, aiding in pore widening and the clearance of clogged pores and comedones. [44]

2.5.2 Nucleases

Deoxyribonucleases (DNases), a category of endonucleases, are specialized enzymes crucial in disrupting the biofilm matrix of *C. acnes*. By cleaving the phosphodiester bonds in the nucleotide chain of the extracellular DNA (eDNA), DNases specifically digest DNA. [7] By degrading eDNA, they inhibit biofilm formation and aid the detachment of existing biofilms. [45]

To improve enzyme penetration through the matrix, delivery via cationic surfactants like liposomes has shown increased effectiveness in eradicating both planktonic and biofilm-forming *C. acnes*. This approach holds promise for enhancing enzyme efficacy in biofilm disruption and combating acne vulgaris. [45, 46]

2.5.3 Lysozymes

Lysozymes, essential antibacterial enzymes in innate immunity, hydrolyze the β-1,4-glycosidic bonds in peptidoglycan polysaccharides, particularly in Gram-positive bacterial cell walls. Recently, lysozymes have emerged as antibiotic substitutes, combating infectious diseases and biofilm formation. [47, 48]

In a 2018 study, researchers investigated the inhibitory capabilities of lysozyme in combination with the circular peptide AS-48. Derived from various *Enterococcus* species, AS-48 demonstrated enhanced efficacy against *C. acnes* when combined with lysozyme, offering a promising alternative for managing acne vulgaris. Utilizing multiple components could further enhance effectiveness, with one component disrupting the biofilm matrix and lysozyme more effectively lysing bacteria embedded within the biofilm. [47, 49]

2.6 Cosmetic Products Regulation

The cosmetic product regulation encompasses various requirements to ensure the protection of human health. These include safety assessments, substance restrictions, designation of responsible persons, Good Manufacturing Practice (GMP), notifications, documentations, labeling and claims, and testing. [50]

A designated responsible person or company must ensure the cosmetic product complies with all relevant obligations. This includes ensuring the product undergoes a safety assessment before being marketed. To perform the necessary lab tests, the responsible person should employ a qualified safety assessor to conduct the product safety assessment. Once completed,

the responsible person can finalize the required documentation – the cosmetic product safety report, which consists of two parts: Part A, covering product safety, and Part B, covering the safety assessment. The regulation also mandates notification via the Cosmetic Products Notification Portal (CPNP). Packaging requirements specify that the container of a cosmetic product must have clearly visible labeling information. [50]

For cosmetic products, following GMP is essential to ensure consistent production and quality control according to standards appropriate for their intended use. GMP includes guidelines for the production, control, storage, and shipment of products. REACH is a legislative framework for the registration, evaluation, authorization, and restriction of chemicals, regulating those manufactured and used in the EU to ensure safety before market introduction. It covers chemicals in their pure form, in mixtures, or as part of products. The General Product Safety Regulation (GPSR), which replaces the General Product Safety Directive (GPSD), provides more detailed requirements for product safety in the EU market. [50]

2.7 Intended work

This thesis intends to explore the use of enzymes as a strategy to combat acne, specifically focusing on their potential to degrade acne biofilms. The study will investigate how enzymes can disrupt the extracellular matrix or lyse the cells within the biofilms.

To conduct this research, it will be necessary to establish methods will for cultivating acne biofilms and for characterizing these biofilms both before and after enzyme treatment. Since the aim is to both disrupt the biofilm and lyse the bacteria within, two different methodologies will be established: one to assess the quantity of biofilm formed, and another to evaluate the viability of the cells residing in the biofilm.

Several enzymes, including proteases, nucleases, and lysozyme, will be tested for their efficacy against *C. acnes* biofilm. Proteases are chosen primarily because they are already used in cosmetics, making them readily available in qualities suitable for cosmetic formulations. Additionally, proteases offer multifunctional benefits for targeting acne, and there is a comprehensive library of these enzymes available at ZymIQ for testing. Proteases vary significantly in substrate specificity, pH dependency, and formulation, which justifies evaluating a diverse panel of different proteases with different properties.

Nucleases are considered for their potential to degrade eDNA within the biofilm matrix, representing another promising enzyme to study. Lysozymes, known for their cell-lysing action

through cell wall disruption, will also be examined. Another related enzyme, lysins, which offer higher bacterial specificity, could be considered but are beyond the scope of this project.

Finally, with the knowledge gained in biofilm studies, the goal is to develop a cream containing the most effective enzyme, alongside other cosmetic ingredients, to offer a gentle yet effective treatment option for individuals seeking alternatives to the comparatively harsh acne treatment regimens available today.

3. Materials and Methods

In the potential development of an enzyme-based formula to combat acne, it is crucial to assess the effects of the enzymes on *C. acnes* biofilms initially.

The biofilm formation process was optimized before testing the enzymes to ensure the most favorable experimental conditions. Once the optimal growth conditions for biofilm formation were determined, the experiment could proceed to enzyme testing. Each enzyme was tested in triplicates of different concentrations to determine the amount required for breaking down the bacterial biofilm. Two assessment methods, the crystal violet assay for biofilm disintegration and the resazurin assay for cell survival, were conducted.

Further evaluations involved exploring whether the enzymes could prevent biofilm formation rather than solely breaking it down. Finally, the selected enzymes were incorporated into a formulation that ensures enzyme stability and user-friendliness. The product was a prototype of what could be put on the market in the future.

The risk assessment can be found in Appendix A.

3.1 Medium preparation

Brain Heart Infusion (BHI) broth powder (Merck, USA) was prepared as recommended by the manufacturer. The medium was transferred to serum bottles, boiled, then flushed with nitrogen. Directly after flushing, the bottles were sealed with a rubber stopper, followed by an aluminum flip cap.

The saline solution was prepared by mixing sodium chloride with distilled water to a concentration of 0.9% (w/v) NaCl. BHI medium, NaCl solution, bottles, pipette tips and other labware were autoclaved at 121°C for 15 min.

3.2 Cultivation of *Cutibacterium acnes* and *Cutibacterium avidum*

When not further specialized, the acneic strain *C. acnes* RT5 (CCUG 1794T) and the specie *C. avidum* (CCUG 36754T) was used, both bacteria were obtained from Culture Collection University of Gothenburg. Glycerol stocks were stored at -80°C. The thawed sample was used to inoculate 15 mL of BHI anaerobically. The bacterial culture tube was filled completely with the media and the *C. acnes* strain, the falcon tube was closed immediately to avoid presence of oxygen. The bacterial culture was then incubated at 37°C for 24 h.

Optical density (OD) of the bacterial culture was measured in a spectrophotometer at 600 nm. OD 0.1 corresponds to ~1 x 10^8 CFU/mL. [51]

3.3 Biofilm formation

The bacterial cell culture was diluted to a concentration of ~10^8 CFU/mL, and the final volume 50 mL. A number of polystyrene 96-well plates (Sarstedt, Sweden) were prepared, one control and the rest containing only bacteria/media solution. In the control plate, rows A and B contained 100 µL of media without bacteria present, while rows C-H included 100 µL of the bacterial inoculum. Rows E-F in the control plate represented buffer control, and rows G-H was the antimicrobial control. A volume of 100 µL inoculum was added into every well of the other plates. The plates were incubated aerobically at 37°C for 4 or 24 h for the cells to adhere to the bottom of the wells.

The media and planktonic cells were carefully removed using a multichannel pipette in the corner of the wells. All wells were cleaned with saline solution 1-3 times before adding 100 µL fresh media into the wells. All plates were put into an anaerobic jar with AnaeroCult (Merck, USA) and incubated anaerobically at 37°C for 24 h. After 24 h the media was removed using a multichannel pipette and replaced with 100 µL fresh media. Plates were incubated for another 24 h.

3.4 Enzyme preparation

Enzyme preparation began with diluting the enzymes, listed in Table 3, to the desired concentration using DPBS (Thermo Fisher, UK). The enzyme tablet tested required a different preparation method: it was first dissolved in 5 mL of distilled water and then placed on a tilting plate until fully dissolved. The solutions were sterilized using a syringe and a 0.22 µm syringe filter. A volume of 250 µL were then transferred in triplicates into the top wells of a 96-well

plate. The remaining wells were filled with 125 µL DPBS. A dilution series was conducted by transferring 125 µL of the enzyme solution from the first row to the second, then from second to third and so forth until all wells contained the desired enzymes.

With a multichannel pipette 50 µL of enzymes were transferred from the enzyme plate to the corresponding row on the bacterial plates along with 50 µL glucose (Millipore, Germany) solution (0.56 g/L) as nutrient source. Plates were then left to incubate aerobically for 4 h at 37°C.

Table 3. List of the enzymes tested in this experiment.

Enzymes for testing
Nuclease I
Nuclease II
Lysozyme
Protease I
Protease II
Protease III
Protease IV
Protease V
Protease VI
Protease VII
Engineered endolysins
Anti-acneic peptide
Enzyme tablet (two glycosidases and one nuclease)

3.5 Crystal violet biofilm eradication assay

After enzymatic incubation, the plates were emptied and rinsed with saline solution (0.9%). Under a fume hood the biofilms were fixed with 100 µL 99% methanol (EMSURE, Germany) for 15 min. The plates were emptied and allowed to evaporate for approximately 5 min. Each well was then filled with 100 µL crystal violet (Thermo Scientific, USA) solution (0.5% w/v). After 20 min incubation, the CV was removed, and the plates were rinsed in a water bath until all excess dye was removed. Finally, 100 µL of acetic acid (33% v/v) (EMSURE, Germany) was added to all wells and incubated for 20 min to dissolve the bound crystal violet. Absorbance at 590 nm was measured using a BioTek Synergy H1 microplate reader (Agilent, USA).

3.6 Biofilm optimization assay

To optimize biofilm formation, a trial was conducted to test various durations for both adhesion and biofilm formation. Five polystyrene 96-well plates were prepared with bacterial cell

culture. Two adhesion periods, 4 h and 24 h were paired with three biofilm formation durations: 24 h 48 h, and 72 h. This resulted in five plate combinations: 4 h adhesion + 24 h biofilm formation; 4 h adhesion + 48 h biofilm formation; 4 h adhesion + 72 h biofilm formation; 24 h adhesion + 24 h biofilm formation; and 24 h adhesion + 48 h biofilm formation. To see if there was any difference in biofilm formation when the media was changed, this was done on row E-H every 24 h on the plates that were incubated for 48 h and 72 h. The combination of 24 h adhesion + 72 h biofilm formation was not assessed due to time constraints. A crystal violet assay was conducted according to section 3.5, to assess the presence of biofilm.

3.7 Cell viability resazurin assay

Cell viability was measured using a resazurin assay. As for the crystal violet the plates were emptied and rinsed with saline (0.9%). Resazurin (Sigma, USA) stock solution (0.02 % w/v) was mixed with saline solution to a final concentration of 0.002%. Each well was filled with 100 µL resazurin solution and incubated for 1 h at 37°C before doing absorbance and fluorescence endpoint measurements with a BioTek Synergy H1 microplate reader.

3.8 Resazurin optimization assay

The cultivated bacteria were transferred to a non-treated polystyrene 96-well plate, with one row containing the original concentration, another row with OD 0.1, and a third row serving as a blank with only resazurin. Resazurin was added to the bacterial rows just before initiating measurements. Kinetic data was collected every minute for 55 min at 37°C using a Multiscan GO microplate reader (Thermo Scientific, USA).

Subsequently, another 96-well plate was prepared with a dilution series of the bacterial culture, starting from an OD of 1.2 and decreasing in increments to OD 0.2, with a final row containing only resazurin as a blank. Resazurin was added just before measurement initiation. Kinetic data was collected at a wavelength of 570 nm and 600 nm every minute for 10 min at 37°C using a Multiscan GO microplate reader.

3.9 Calculations

To calculate the biofilm eradication by the enzymes, Equation 1 was used based on absorbance (A) values. A_{sample} represents the mean value of the triplicates for each concentration. $A_{positive}$ and $A_{negative}$ are the mean values of all wells containing the positive and negative controls, respectively. The positive control contained the fully formed biofilm, while the negative

control contained no cells, therefore by substrating the negative control values from the positive control values, the backround noise was removed.

$$Biofilm\ eradication\ = 100 \cdot \left(1 - \left(\frac{A_{sample} - A_{negative}}{A_{positive} - A_{negative}}\right)\right) \quad (1)$$

3.10 Formulation of potential product

Water and glycerol (VWR, Belgium) were weighed and mixed with a propeller until the mixture was well blended. Then the Xanthan (BASF, Germany) was added, and the mixture was homogenized at 10,000 rpm until it thickened, and the Xanthan was evenly distributed. The Tris/HCl buffer with $MgCl_2$ (in house/ZymIQ, Sweden) was prepared and added to the mixture along with Xylitol (Sigma, USA), Pentylene glycol (Evinok, Germany), and Niacinamide (DSM, Switzerland). These ingredients were blended in with the propeller. In a separate container, Caprylic/capric triglyceride (Jan Dekker, Netherlands) and a commercial mixture of emulsifiers composed of Polyglyceryl-3 cocoate, Hydrogenated lecithin and Lecithin (Sharon, Italy) were mixed at 40°C until it was fully dissolved. This mixture was then added to the main mixture and homogenized at 10,000 rpm until a uniform emulsion was formed. The anti-acneic peptide and nuclease II were added, and the mixture was stirred with a propeller for 30 min. Finally, the mixture was distributed into 30 mL bottles, and 1 mL was reserved for further testing.

4. Results

4.1 Testing the impact of various enzymes on preformed biofilms – Experiment I

The following results are from Experiment I, while the remaining experimental results can be found in Appendix B.

The cell suspension measured an OD_{600nm} of 0.64 after 24 h of incubation in BHI medium and was diluted to an OD_{600nm} of 0.1 before plating.

To study the impact of enzymes on *C. acnes* biofilms, these were established in the wells of three 96-well plates. As described previously [34, 52], 4 h were selected for cell adhesion, 24 h for biofilm propagation, and another 24 h for enzyme treatment. Then CV and resazurin were used to characterize the biofilms after enzyme treatment. Table 4 illustrates the values on the controls for each assay.

Table 4. Fluorescence to the left (resazurin) and absorbance to the right (CV) of the control plate. Row A-B are negative controls, C-D positive controls, E-F buffer controls and G-H antibiotic control (Carbenicillin).

Plate 1	1	2	3	4	5	6	7	8	9	10	11	12
A	2706	2826	2780	2883	2476	2545	0.071	0.061	0.07	0.072	0.076	0.087
B	2516	2570	2371	2564	2227	2410	0.061	0.068	0.064	0.078	0.074	0.06
C	22602	20398	17886	17593	15365	15540	0.097	0.087	0.087	0.077	0.069	0.075
D	27942	26088	20719	23700	25301	21775	0.122	0.111	0.116	0.125	0.108	0.093
E	12769	16080	13339	10512	13440	11480	0.083	0.093	0.085	0.099	0.086	0.081
F	23821	18901	17555	18863	15075	15864	0.086	0.085	0.085	0.087	0.098	0.096
G	2424	2524	2350	2472	2409	2357	0.078	0.066	0.07	0.079	0.077	0.07
H	2484	2600	2371	2603	2389	2324	0.075	0.087	0.066	0.063	0.069	0.073
	Resazurin assay						**Crystal violet assay**					

Plate one contained several positive and negative controls and was used to evaluate the feasibility of the approach.

As can be seen from the data in columns 1 to 6, here was an approximately 4-to-10-fold increase in fluorescence signal in the positive controls, indicating the formation of the biofilm. The fluorescence signal was somewhat lower (approximately by 30%) in wells inoculated in the presence of buffer (glycerol dilution buffer and PBS, see Appendix C for detailed information on their composition).

The results after staining the biofilm with CV indicate (in contrast to the resazurin data) that biofilm formation was very limited (columns 7-12). Absorption at 590 nm showed only a 1,4-fold increase in the positive controls.

The other two plates were incubated with six different enzymes (one nuclease, one lysozyme, and four proteases), an anti-acne peptide, and an enzyme tablet. The enzyme/peptide concentration was varied to determine the dose-dependent effect on the biofilm. After treatment, the plates were stained with resazurin and CV respectively. The visible results for the resazurin assay are shown with a picture of plate one in Figure 7, the corresponding fluorescent data are provided in Table 5.

Figure 7 2. Image of a 96-well plate after resazurin staining, showing cell viability after 24 h of enzyme treatment and 40 min of incubation with resazurin. The enzyme concentrations decrease from top to bottom, and the wells are organized as follows: Nuclease I (A1:D3), Lysozyme I (A4:D6), Protease I (A7:D9), Protease II (A10:D12), Enzyme tablet (E1:H3), Protease III (E4:H6), Protease IV (E7:H9), and Anti-acneic peptide (E10:H12). The color ranges from blue, indicating low cell viability, to light pink, indicating high cell viability.

Differences in resazurin/resorufin ratio were clearly visible to the naked eye, dark blue wells (associated with low fluorescence) indicate the absence of metabolically active cells, while pink wells (associated with high fluorescent signal) show their presence. Thus, if an enzyme can eradicate the biofilm and kill the cells residing in the biofilm, wells will present in blue rather than pink.

Results concerning dose dependency were difficult to interpret. Ideally, one would expect that the well color changes from blue to pink (i.e. from low to high fluorescents) as the enzyme concentrations decrease. Looking at Table 5, this was only seen with one of the enzymes tested, namely Protease II (columns 10-12 and lanes A-D). Unexpectedly, Protease IV showed the opposite behavior. As for the enzyme tablet (E1:H3), it looked like all biofilm had been removed. The opposite was seen for Protease III (E4-H6), where almost all resazurin had been reduced to resorufin, giving the light pink color, indicating that viable cells are present.

Table 5. Flouresence endpoint values from the resazurin assay after treating *C. acnes* with enzymes. Measurements were made at a wavelength of 450 nm , with excitation at 540 nm and emission at 590 nm, after 40 min of incubation with resazurin. The enzyme concentrations decrease from top to bottom, and the locations are as follows: Nuclease I (A1:D3), Lysozyme I (A4:D6), Protease I (A7:D9), Protease II (A10:D12), Enzyme tablet (E1:H3), Protease III (E4:H6), Protease IV (E7:H9), and Anti-acneic peptide (E10:H12).

Plate 2	1	2	3	4	5	6	7	8	9	10	11	12
A	16902	17161	21674	14426	11625	13983	27704	27946	29088	19203	3878	15243
B	4227	24443	26112	15433	12962	14895	28391	24455	31639	22798	21919	26984
C	20480	21727	21595	28036	23881	19611	12197	22697	19989	35970	44100	36265
D	13520	16047	14690	17825	16647	18392	26575	25521	28892	27765	29261	22282
E	16671	10630	5890	36450	21126	25519	27684	27888	20319	22082	27244	36012
F	4395	5853	7412	21766	16196	20655	23594	26995	28547	32428	31164	35350
G	7436	10391	16644	12965	15917	7670	21045	22538	26443	34628	31042	37832
H	6189	5531	7000	26517	14351	19631	16238	16081	23085	30407	28769	29191

The crystal violet results were also challenging to interpret in terms of dose dependency. Ideally, higher enzyme concentrations would lead to lower absorbance values, indicating biofilm removal. However, as shown in Table 6, this trend was not observed for any of the enzymes tested. Instead, biofilm degradation appeared to occur randomly. The washing step appeared to discard the biofilm before addition of enzymes.

Table 6. Absorbance endpoint values from the CV assay after treating *C. acnes* with enzymes. Measurements were made at a wavelength of 590 nm. The enzyme concentrations decrease from top to bottom, and the locations are as follows: Nuclease I (A1:D3), Lysozyme I (A4:D6), Protease I (A7:D9), Protease II (A10:D12), Enzyme tablet (E1:H3), Protease III (E4:H6), Protease IV (E7:H9), and Anti-acneic peptide (E10:H12).

Plate 3	1	2	3	4	5	6	7	8	9	10	11	12
A	0.112	0.074	0.09	0.11	0.079	0.105	0.118	0.095	0.112	0.071	0.079	0.093
B	0.089	0.095	0.079	0.079	0.104	0.105	0.078	0.074	0.069	0.056	0.075	0.1
C	0.078	0.096	0.074	0.071	0.072	0.08	0.062	0.073	0.082	0.079	0.076	0.099
D	0.086	0.078	0.073	0.074	0.101	0.105	0.074	0.15	0.076	0.08	0.089	0.152
E	0.074	0.081	0.073	0.084	0.076	0.074	0.088	0.069	0.084	0.083	0.065	0.082
F	0.093	0.081	0.061	0.085	0.102	0.081	0.069	0.139	0.152	0.092	0.084	0.098
G	0.081	0.084	0.071	0.069	0.082	0.076	0.085	0.102	0.13	0.108	0.093	0.091
H	0.076	0.083	0.075	0.074	0.07	0.073	0.078	0.084	0.116	0.086	0.086	0.087

The formula for calculating biofilm eradication was used for the various concentrations of enzymes used in this experiment. The biofilm decrease from the crystal violet assay performed during Experiment 1 are presented in Table 7, the calculations were done according to Equation 1. The reduction in biofilm did not exhibit a linear relationship with enzyme concentration.

Table 7. Variation in percentage for decreased biofilm for the various enzymes.

Enzyme	Nuclease I	Lysozyme	Protease I	Protease II	Enzymatic tablet	Protease III	Protease IV	Anti-acneic peptide
Decrease (%)	19 +/- 2 %	-3 +/- 2 %	-41 +/- 1 %	60 +/- 1 %	78 +/- 0 %	71 +/- 1 %	62 +/- 1 %	76 +/- 1 %
	35 +/- 1 %	5 +/- 1 %	87 +/- 0 %	75 +/- 2 %	70 +/- 2 %	29 +/- 1 %	-84 +/- 4 %	22 +/- 1 %
	54 +/- 1 %	85 +/- 0 %	92 +/- 1 %	46 +/- 1 %	69 +/- 1 %	80 +/- 1 %	-31 +/- 2 %	0 +/- 1 %
	67 +/- 1 %	14 +/- 2 %	-10 +/- 4 %	-36 +/- 4 %	71 +/- 0 %	92 +/- 0 %	17 +/- 2 %	40 +/- 0 %

Further attempts were executed but these did not yield definitive results regarding the enzymatic effect on *C. acnes* biofilm. Fluorescence and absorbance values from these experiments can be seen in Appendix B.

4.2 *C. acnes* biofilm formation optimization

From the above results, the CV based biofilm assay should be optimized further, and possibly the biofilm formation needs to be improved as well. Therefor a new set of experiments was carried out focusing on biofilm formation and CV staining.

To find the optimal conditions for *C. acnes* biofilm formation, the effects of adhesion time, biofilm formation time, and medium changes during biofilm formation were investigated.

Adhesion was allowed to proceed for either 4 or 24 h, and biofilm formation was allowed for 24, 48, or 72 h. For biofilm formation times were prolonged more than 24 h and the impact of exchanging the medium every 24 h was also assessed.

The CV assay was used to determine the amount of biomass formed, starting from an inoculum of 100 µL of *C. acnes* suspension diluted from an OD of 0.86 to an OD of 0.1.

Quantitative data from this experiment are presented in Figure 8, showing the absorbance mean values measured at 590 nm from the crystal violet assay. These values reflect different adhesion and biofilm formation periods at a cell concentration of OD 0.1. The combinations of 4 h adhesion followed by 48 and 72 h of biofilm formation, with media changes every 24 h, showed the highest absorbance values, approximately OD of 1. Conversely, the lowest absorbance values were observed in the 4 h + 24 h and 4 h + 72 h combinations without media changes.

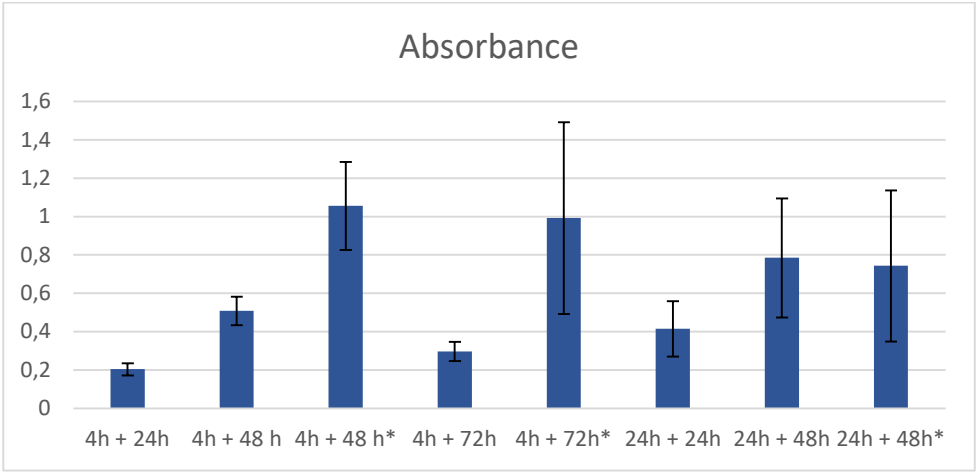

Figure 83. Diagram illustrating the absorbance mean values of biofilms for different time combination. The ones marked with (*) have had a media change every 24 h.

Adhesion time, incubation time, and medium exchange profoundly affected the amount of biofilm formed. Differences in biofilm amounts were clearly visible by the naked eye (Figures 9 and 10). It is worth mentioning that the color intensity was stronger in wells where the medium was exchanged during incubations (Figure 9, rows E and F).

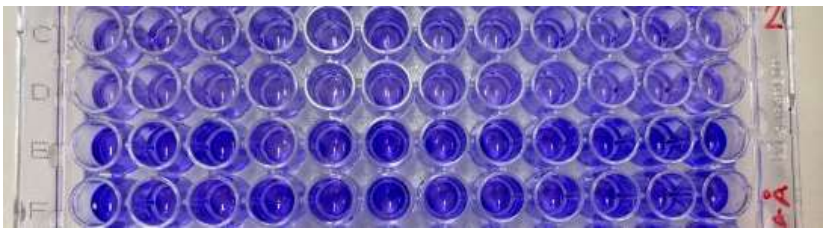

Figure 94. Image of a 96-well plate (Plate 2) from a crystal violet assay, showing biofilm formation after an initial 4 h adhesion time followed by 48 h biofilm growth. In rows E-F, the media was changed every 24 h.

Figure 105. Image of a 96-well plate (Plate 1) from a crystal violet assay showing minimal biofilm formation after a 4 h adhesion and a 24 h biofilm growth period without any media changes.

4.3 Resazurin optimization assay for *C. acnes*

The conversion of resazurin to resorufin is time dependent and therefore the selection of incubation time is crucial. If the incubation time is too long the substrate might be completely consumed, independent of the amount biofilm present. This is what was seen in Experiment 1 when investigating the impact of protease III on the biofilm.

To determine the incubation time required for different cell concentrations of *C. acnes* to metabolize resazurin, a resazurin assay was conducted. Kinetic measurements were taken using a microtiter plate reader to monitor the conversion of resazurin to resorufin. These measurements were performed on planktonic cells at various concentrations, with the highest concentration representing a biofilm mass approximately 10 times that of the inoculum, which previous experiments have shown to be a reasonable amount.

After 55 min, at a concentration of OD 1, the resazurin has been fully metabolized into resorufin, indicating much higher total metabolic activity. In contrast, at a concentration of OD 0.1 the cells are showing some metabolic activity (Figure 11).

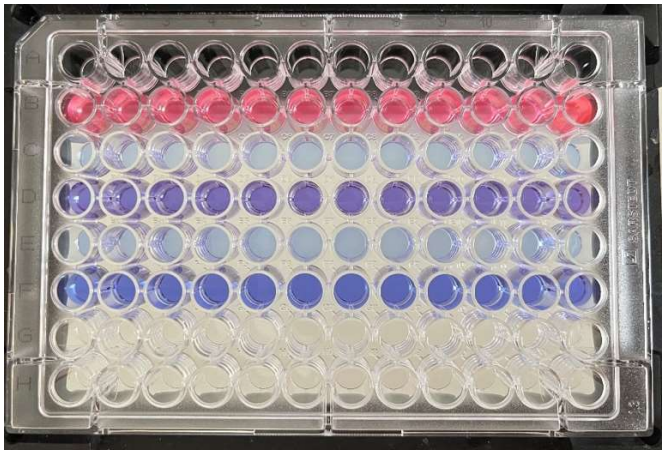

Figure 116. Image of a 96-well plate after a 55 min resazurin assay on planktonic cells. Row B (OD 1) shows significant color change indicating high metabolic activity. Row D (OD 0.1) shows less activity, and row F, the control with only resazurin, shows the baseline color.

Figure 12 illustrates the visible results of a 10 min resazurin assay, highlighting the relationship between cell concentration and overall metabolic activity. The assay shows a notable shift in metabolic activity between OD 0.4 and OD 0.6, indicating that resazurin conversion is closely tied to cell density and incubation time.

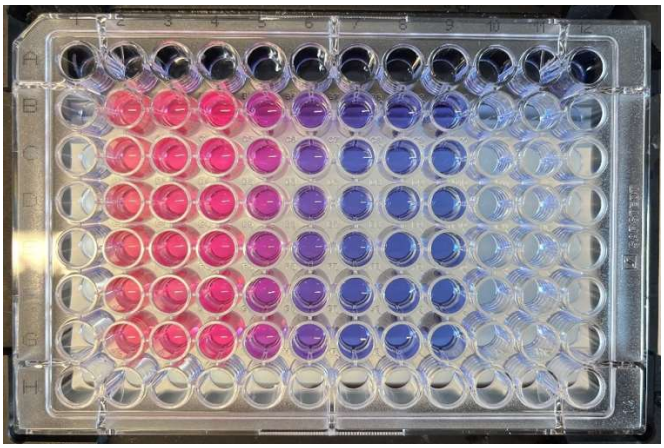

Figure 127. Image of a 96-well plate after a 10 min resazurin assay. Column 2, with the highest cell concentration (OD 1.2), shows the most color change, indicating high metabolic activity. Contrastingly, column 8, with the lowest cell concentration (OD 0.1), displays minimal color change. The gradient of color from left to right reflects decreasing cell concentration and metabolic activities. Column 9 is the control containing only resazurin, showing the baseline color.

Figures 13 and 14 display the rate of resazurin usage and production of resorufin at different cell concentrations. These figures illustrate the metabolic activity over time, with specific focus on the relationship between the substrate (resazurin) and the product (resorufin). This experiment aims to determine the optimal wavelength and incubation time for performing endpoint measurements.

In Figure 13, the time course of resazurin conversion of cells at two different optical densities (OD) are represented. The left diagram shows a cell concentration of OD 1.2, where the turning point for resazurin metabolism occurs almost immediately, at around 1 min. After 8 min,

resorufin continues to metabolize into the byproduct hydroresorufin, as indicated by the change in slope. This suggests that resorufin is not a stable product, and the reversible reaction between resorufin and hydroresorufin affects the measurements. The right diagram illustrates a cell concentration of OD 0.1, where the metabolic rate was much lower, and no turning point was observed even after 20 min.

Figure 14 depicts the metabolic rate at an OD of 0.6. The turning point for resazurin metabolism at this concentration occurs after approximately 9 min.

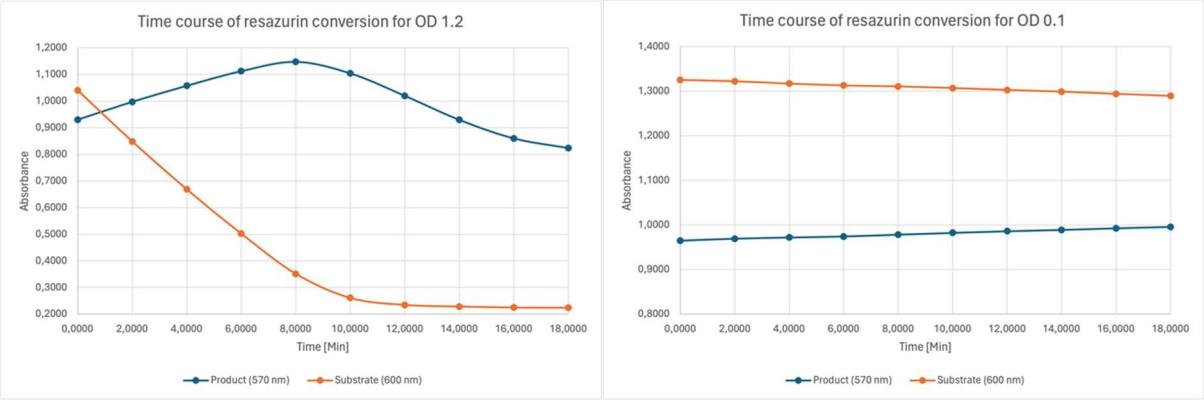

Figure 138. Diagrams showing the time course for conversion of resazurin to resorufin at two different ODs. The blue line represents the substrate (resazurin) being metabolized over time, and the orange line represents the product (resorufin) being produced over time. The left diagram corresponds to an OD of 1.2, where the turning point occurs around 1 min. The right diagram corresponds to an OD of 0.1, showing a much lower metabolic rate with no turning point after 20 min.

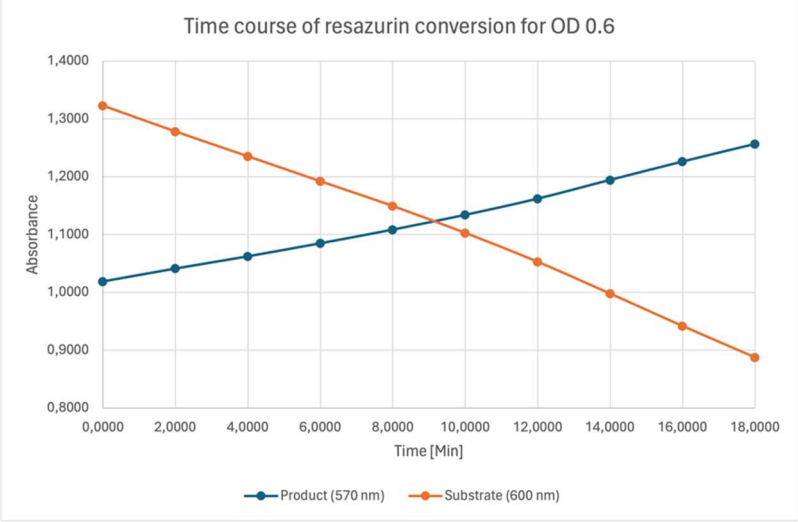

Figure 149. Diagram showing the metabolic rate of resazurin to resorufin at an OD of 0.6. The blue line represents the substrate (resazurin) being metabolized over time, and the orange line represents the product (resorufin) being produced over time. The turning p point occurs after approximately 9 min.

Upon examining the diagram in Figure 15, an initial rate determination time of 8 min was selected, after this time it could not be guaranteed that the rate was linear.

Subsequently, kinetic measurements were made at two different wavelengths: 570 nm, and 600 nm. The 600 nm wavelength measures the substrate, 570 nm measures the product, as illustrated in Figure 15. The rate data are shown as positive values, to facilitate comparison. As shown in the figure, 600 nm was the optimal wavelength for this assay, as it showed the greatest response.

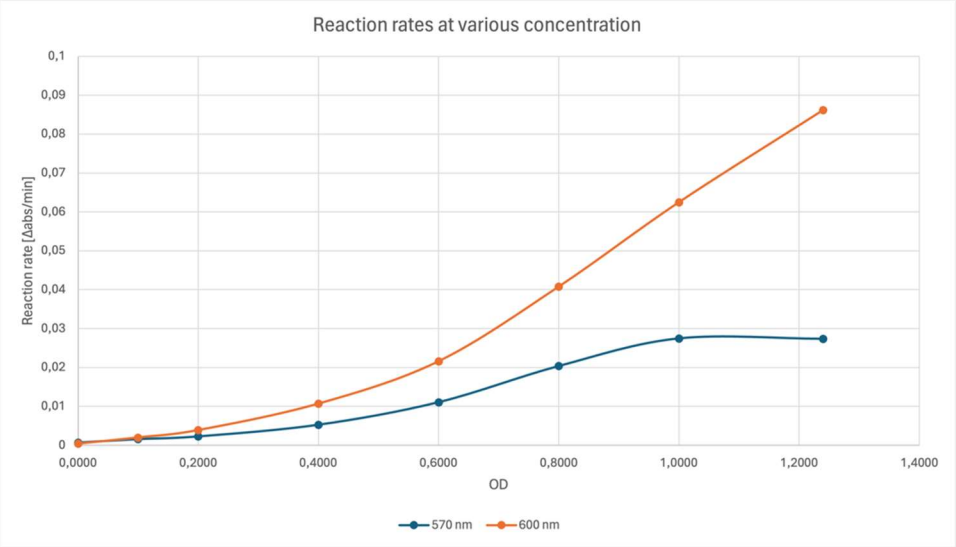

Figure 1510. Graph illustrating kinetic measurements at 570 nm (orange line), and 600 nm (green line). The Y-axis represents the reaction rate, and the X-axis shows the different concentrations. The 600 nm wavelength measures the substrate, 570 nm measures the product. The decrease in substrate has been mirrored to approximate the increase in product for easier comparison.

4.4 Enzymatic efficiency of Nuclease II

With a deeper understanding of biofilm formation and evaluation, several new experiments were made to investigate the impact of enzymes on acne biofilms. Based on previous studies, specific modifications were implemented: cell adhesion occurred over 4 h, followed by 48 h of biofilm propagation with a medium change after the initial 24 h, and another 4 h for enzyme incubation in the presence of glucose (instead of BHI). The CV assay was used to characterize the biofilms post-enzyme treatment, focusing on Nuclease II which showed promising results.

Two experiments were performed similar to Experiment I, both involving Nuclease II tested in eight different concentrations. After 24 h of incubation in BHI medium, the cell suspensions reached ODs of 1.05 and 1.40, respectively. Prior to inoculation, these suspensions were diluted to an OD of 0.315 for Experiment 4 and 0.2 for Experiment 5. Figure 16 visually illustrates the effect of Nuclease II on *C. acnes* biofilms in Experiment 4 and 5.

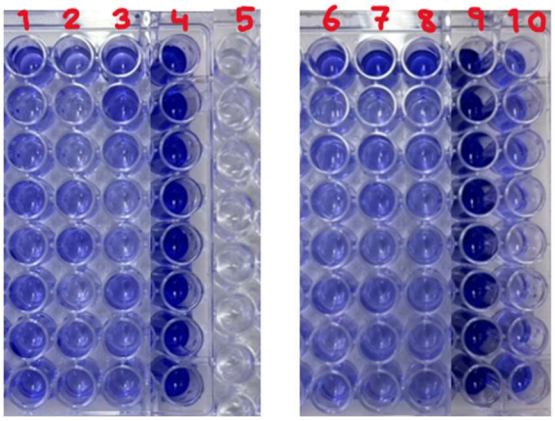

Figure 1611. Image of two 96-well plates from CV assays performed on different occasions, showing biofilm formation after an initial 4 h adhesion time followed by 48 h biofilm growth, with media changed after the initial 24 h, and 4 h enzyme treatment. Nuclease II was tested in degreasing concentrations in columns 1-3 for Experiment 4 and columns 6-8 for Experiment 5. Positive controls for the first and second experiments are in columns 4 and 9, respectively, and negative controls in columns 5 and 10, respectively.

Upon examination, a clear difference was visible between the enzyme-treated wells and the untreated wells. In Experiment 4, the negative control behaved as expected. However, in the second experiment, the negative control exhibited some contamination, indicated by the blue shade in the wells. Surprisingly, higher enzyme concentrations did not lead to greater biofilm breakdown in these experiments, complicating the interpretation of dose dependency.

Analyzing the absorbance values from the plates, Experiment 4 demonstrated a 22-39% reduction in biofilm compared to the positive and negative control. Unfortunately, Experiment 5 yielded overflow measurements, rendering calculations impossible due to excessively high absorbance values in the CV assay. Nevertheless, the visible effect of the enzyme, as shown in Figure 16, remained evident for both experiments. Notably, the reduction in biofilm did not follow a linear relationship with enzyme concentration.

4.5 Efficiency of Anti-acneic peptide

Further testing was conducted on the anti-acneic peptide by adding it prior to the 21 h adherence and 43 h biofilm formation periods to assess its effect in biofilm prevention. A CV assay was performed to evaluate the efficacy of the peptide, which showed a decrease in biofilm of 49% at the highest peptide concentration and 16% at the lowest concentration. The lowest decrease (6%) occurred at the second lowest concentration.

4.6 Biofilm eradication by the enzymes

Equation 1 was used to calculate biofilm eradication for various concentrations of six different enzymes used in Experiment 3 and 4. The decrease in biofilm, based on absorbance values from the crystal violet assays, is presented in Figure 17. The decrease was expected to be proportional between biofilm eradication and decreasing enzyme concentration, however, it is evident that there were no linear relationships based on dosages. Furthermore, there was no consistency between the two different experiments, even though they were performed similar.

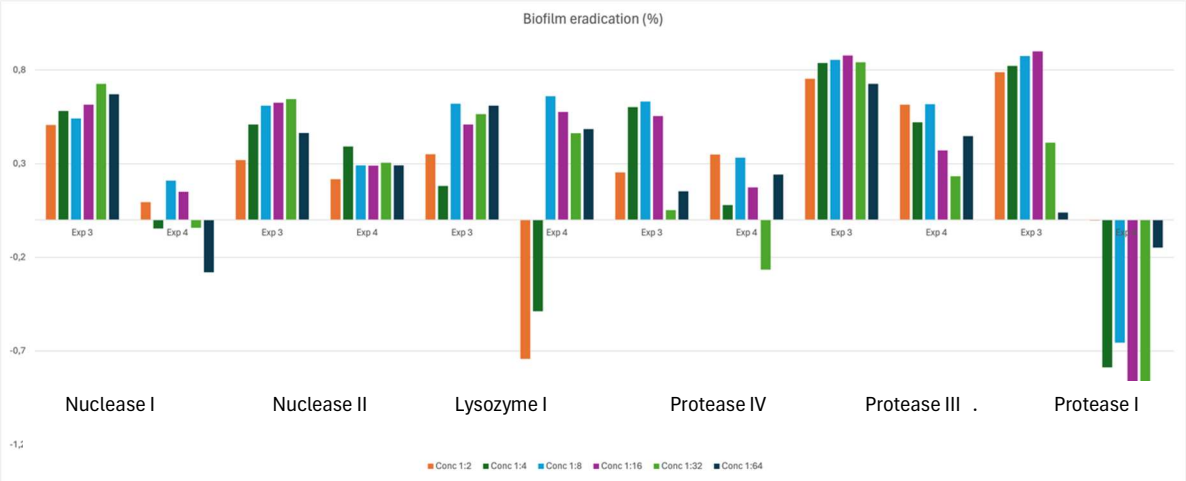

Figure 1712. Biofilm eradication in percentage for six different enzymes with varying concentrations. Each cluster assemble one experiment, two experiments are shown for each enzyme. Every color represents a concentration.

4.7 Product

A product was developed using an existing face moisturizer from ZymIQ as inspiration for the base, incorporating Nuclease II, the Anti-acneic peptide, and niacinamide, all of which have shown potential effects on acneic *C. acnes* strains and their biofilm formation. Figure 18 shows an image of the final developed product. More information about the ingredients and usage of this proposed product can be found in Appendix D.

Figure 1813. Image of the final ClearZyme Puryfying Face Gel sample, packaged in 30 mL bottles. The batch number is ALMF37, and the label includes the ingredient list and the company's address.

5. Discussion

The study of enzymatic degradation of *C. acnes* biofilms offers promising insights into potential acne treatments. However, the experiments revealed significant challenges and inconsistencies, highlighting the complexities of biofilm formation and enzyme activity. This discussion explores the results and issues encountered during these experiments, examining the factors that may have influenced the outcomes and suggesting future research directions.

The first experiment (Experiment 1) initially appeared promising, with visible differences between the effects of various enzymes. However, a detailed analysis of the data revealed several issues. Overall, the results did not show a clear connection with specific enzymes and their ability to disrupt the biofilm. Several factors could explain this lack of correlation: 1) the conditions might not have been conductive for *C. acnes* to form a stable biofilm, resulting in no biofilm to eradicate, 2) the environment may not have been favorable for the enzymes to function effectively, 3) the incubation time might not have been sufficient for the biofilm to mature.

One significant issue was that data from CV assay and the resazurin assay were not aligned when comparing positive and negative results. While the resazurin assay showed tenfold increase in signal, the CV assay indicated only a 1.4-fold increase in biomass. This discrepancy could be due to several factors, such as the biofilm desorbing during the CV staining procedure or the resazurin assay overestimating biofilm formation due to non-linear responses from the fluorescence measurements. The time and cell concentration dependent response of the resazurin assay was therefore investigated. The results indicated some deviation from linearity in the absorption measurements, when assessing the number of active cells by determining the rate in resazurin conversion. Also, it was seen clearly that the formation of hydroresorufin impacted the results leading to an underestimation of resorufin formed. These measurements were done on planktonic cells of *C. acnes* and may not be directly applicable to the biofilm measurements. However, the results indicated that the analysis conditions chosen in the first experiment were appropriate and useful for monitoring the presence of metabolically active cells in biofilms in which the number of metabolically active cells varies up to10-fold. The biofilm optimization assay and the resazurin assay investigation yielded valuable insights, but unfortunately, it was still very difficult to obtain reliable data in subsequent enzyme studies.

Studies on biofilm formation resulted in optimized conditions, yielding biomass amounts comparable to the increase in metabolically active cells. However, the analytical error was rather high and unexplained reasons for why longer incubation times did not yield more biofilm persisted. Problems with reproducibly forming biofilms likely remained, although special care was taken in subsequent experiments not to remove the biofilm during formation and degradation. Possibly, the biofilm was not mature and stable enough to adhere strongly to the plates. To prevent biofilm elimination, washing steps were performed only after adhesion in Experiment 5, though this might have resulted in planktonic cells remaining on the plates. This, in turn, resulted in absorbance values outside the linear region. Therefore, these values cannot be used to calculate biofilm eradication, or to draw any further conclusions. Additionally, the visible biofilm may have only reached the microcolony phase, making it susceptible to removal by mechanical forces.

Likely, the conditions for growing biofilms in the laboratory were more favorable than those on the skin. On the skin, nutrients are limited, and *C. acnes* relies on glycerol-containing sebum for proliferation. Additionally, factors such as oxygen presence disrupt *C. acnes* growth on the skin. The experiments used BHI medium, providing a great source of dextrose carbon for the bacteria. Consequently, the cell density in the experiments reaches up to 100 times higher levels, at 10^8 CFUs/cm^2, compared to 10^6 CFUs/cm^2 [53] on the skin.

In Experiment I, the resazurin assay indicated that both nuclease and lysozyme enzymes reduced the number of metabolically active cells. While nuclease likely diminished the biofilm, lysozyme had an impact on the number of viable cells. However, this assay could not determine enzymatic activity against biofilm, as non-metabolic cells do not necessarily mean no biofilm.

Previous studies have demonstrated that proteases can effectively eradicate bacterial biofilms [7], making them an obvious choice for investigation. However, in this study, significant *C. acnes* biofilm eradication by proteases was not observed. The primary issue arose from inconsistent results across weekly experiments. While inhibition by protease enzymes was evident in some weeks, it was absent in others, rendering the results unreliable due to its inconsistency. Consequently, proteases may have a more substantial impact on biofilms than suggested by these findings. To explore this further, glucose replaced BHI in the last three experiments, although the effect of this change on enzymatic activity remained unclear. Additionally, the buffer was changed from PBS to DPBS (see Appendix C) to provide essential minerals like magnesium and calcium, required for certain enzymes to function.

In terms of dose dependency, higher enzyme concentrations did not consistently lead to greater biofilm disruption as expected. Most experiments showed no clear correlation between enzyme concentration and biofilm degradation, which is quite confounding. This inconsistency is clearly illustrated in Figure 17, where the highest concentration should correspond to the highest bar, yet there is significant variation regardless of concentration. One possible factor influencing these results could be contamination of the negative controls, which would give unreliable results. However, this does not fully explain the lack of consistent pattern, leaving this issue unresolved.

Given the slightly promising results with nucleases in eradicating *C. acnes* biofilm, a formulation containing nuclease was developed, providing a foundation for a potential market product. The product also contained an anti-acneic peptide, that previously has been proven good against acne by inhibiting the adhesion of *C. acnes* within the hair follicle. Lastly it will contain niacinamide, known for reducing sebum secretion. The concentrations used were based on usage recommendations from the producer companies. Future research on the enzyme efficacy will allow concentration adjustments. Before market entry, dermatological tests and compliance with cosmetic product regulations are necessary.

To further investigate biofilm eradication abilities of enzymes, a method for optimizing the biofilm formation needs to be established. Without a clear biofilm to target, it is impossible to determine if enzymes are effective or if biofilm absence is due to other reasons.

6. Conclusion

Acne is a widespread disease with currently limited treatment options, causing suffering for millions of predominantly young individuals. Our studies on the factors contributing to acne have identified several promising approaches involving enzymes to combat this condition. One possible strategy is the breakdown of acne biofilms through the degradation of biofilm matrix components, which are crucial for maintaining the structural integrity of the biofilm.

However, demonstrating the efficacy of enzymes in degrading acne biofilms has proven to be more challenging than anticipated. While there are indications that nucleases may aid in the degradation of *C. acnes* biofilms, further research is necessary to confirm their effectiveness.

7. Future perspectives

Future studies should aim to optimize in vitro biofilm formation and identify components of the extracellular matrix, for specifically targeted strategies. Monitoring the breakdown of these components upon enzyme treatment could provide valuable tools for assessing biofilm maturation and degradation. Another potential focus area would be the study of enzymes on various acnes strains to evaluate eventual differentiation between acneic and non-acneic strains.

Such research could pave the way for clinical trials to establish enzymes as a viable treatment option for acne patients.

8. References

1. Mallikarjun Vasam, Satyanarayana Korutla, Bohara RA. Acne vulgaris: A review of the pathophysiology, treatment, and recent nanotechnology based advances. Biochemistry and Biophysics Reports. 2023 Dec 1;36:101578–8.

2. Coenye T, Spittaels KJ, Achermann Y. The role of biofilm formation in the pathogenesis and antimicrobial susceptibility of Cutibacterium acnes. Biofilm. 2021 Dec;100063.

3. Huemer M, Mairpady Shambat S, Brugger SD, Zinkernagel AS. Antibiotic resistance and persistence—Implications for human health and treatment perspectives. EMBO reports [Internet]. 2020 Dec 3;21(12). Available from: https://www.embopress.org/doi/full/10.15252/embr.202051034

4. Kanwar IL, Haider T, Kumari A, Dubey S, Jain P, Soni V. Models for acne: A comprehensive study. Drug Discoveries & Therapeutics [Internet]. 2018;12(6):329–40. Available from: https://pubmed.ncbi.nlm.nih.gov/30674767/

5. Kostakioti M, Hadjifrangiskou M, Hultgren SJ. Bacterial Biofilms: Development, Dispersal, and Therapeutic Strategies in the Dawn of the Postantibiotic Era. Cold Spring Harbor Perspectives in Medicine. 2013 Apr 1;3(4):a010306–6.

6. O'Neill AM, Gallo RL. Host-microbiome interactions and recent progress into understanding the biology of acne vulgaris. Microbiome. 2018 Oct 2;6(1).

7. Wang S, Zhao Y, Breslawec AP, Liang T, Deng Z, Kuperman LL, et al. Strategy to combat biofilms: a focus on biofilm dispersal enzymes. npj Biofilms and Microbiomes [Internet]. 2023 Sep 7;9(1). Available from: https://www.ncbi.nlm.nih.gov/pmc/articles/PMC10485009/

8. Chernoff KA, Zaenglein AL. Acne and Other Disorders of the Pilosebaceous Unit [Internet]. 23rd ed. Kline MW, editor. Access Medicine. New York, NY: McGraw-Hill Education; 2018 [cited 2024 May 28]. Available from: https://accesspediatrics.mhmedical.com/content.aspx?bookid=2126§ionid=181401326

9. Mayslich C, Grange PA, Dupin N. Cutibacterium acnes as an Opportunistic Pathogen: An Update of Its Virulence-Associated Factors. Microorganisms [Internet]. 2021 Feb 2;9(2):303. Available from: https://www.mdpi.com/2076-2607/9/2/303/pdf

10. Webster GF, Rawlings AV. Acne and Its Therapy [Internet]. Google Books. CRC Press; 2007 [cited 2024 May 28]. Available from: https://books.google.se/books?hl=sv&lr=&id=sx_cua_GYS4C&oi=fnd&pg=PA9&dq=pilosebaceous+unit&ots=1EpdfoAi6-&sig=iBEgTiet6eChA5vGRJvIId2mdVs&redir_esc=y#v=onepage&q=pilosebaceous%20unit&f=false

11. Makrantonaki E, Ganceviciene R, Zouboulis CC. An update on the role of the sebaceous gland in the pathogenesis of acne. Dermato-Endocrinology [Internet]. 2011 Jan;3(1):41–9. Available from: https://www.ncbi.nlm.nih.gov/pmc/articles/PMC3051853/

12. Martel JL, Badri T. Anatomy, Hair Follicle [Internet]. Nih.gov. StatPearls Publishing; 2019. Available from: https://www.ncbi.nlm.nih.gov/books/NBK470321/

13. Kong HH. Skin microbiome: genomics-based insights into the diversity and role of skin microbes. Trends in Molecular Medicine. 2011 Jun;17(6):320–8.

14. Brüggemann H, Salar-Vidal L, Gollnick HPM, Lood R. A Janus-Faced Bacterium: Host-Beneficial and -Detrimental Roles of Cutibacterium acnes. Frontiers in Microbiology. 2021 May 31;12.

15. Lambrechts IA, Nuno de Canha M, Lall N. Hyperkeratinization - an overview | ScienceDirect Topics [Internet]. www.sciencedirect.com. Available from: https://www.sciencedirect.com/topics/medicine-and-dentistry/hyperkeratinization

16. Ramli R, Malik AS, Hani AFM, Jamil A. Acne analysis, grading and computational assessment methods: an overview. Skin Research and Technology. 2011 May 24;18(1):1–14.

17. Marks JG, Miller MD JJ. Comedo - an overview | ScienceDirect Topics [Internet]. www.sciencedirect.com. [cited 2024 May 28]. Available from: https://www.sciencedirect.com/topics/nursing-and-health-professions/comedo

18. Fox L, Csongradi C, Aucamp M, du Plessis J, Gerber M. Treatment Modalities for Acne. Molecules [Internet]. 2016 Aug 13;21(8):1063. Available from: https://www.ncbi.nlm.nih.gov/pmc/articles/PMC6273829/

19. Callender VD, Baldwin H, Cook-Bolden FE, Alexis AF, Stein Gold L, Guenin E. Effects of Topical Retinoids on Acne and Post-inflammatory Hyperpigmentation in Patients with Skin of Color: A Clinical Review and Implications for Practice. American Journal of Clinical Dermatology. 2021 Nov 9;

20. Ahle CM, Feidenhansl C, Brüggemann H. Cutibacterium acnes. Trends in Microbiology [Internet]. 2022 Oct 31;0(0). Available from: https://www.cell.com/trends/microbiology/fulltext/S0966-842X(22)00289-X?rss=yes

21. Teramoto K, Okubo T, Yamada Y, Sekiya S, Iwamoto S, Tanaka K. Classification of *Cutibacterium acnes* at phylotype level by MALDI-MS proteotyping. Proceedings of the Japan Academy Series B, Physical and biological sciences. 2019 Dec 11;95(10):612–23.

22. Dréno B, Pécastaings S, Corvec S, Veraldi S, Khammari A, Roques C. Cutibacterium acnes (Propionibacterium acnes) and acne vulgaris: a brief look at the latest updates. Journal of the European Academy of Dermatology and Venereology. 2018 Jun;32:5–14.

23. Fitz-Gibbon S, Tomida S, Chiu BH, Nguyen L, Du C, Liu M, et al. Propionibacterium acnes strain populations in the human skin microbiome associated with acne. The Journal of investigative dermatology [Internet]. 2013 Sep 1;133(9):2152–60. Available from: https://www.ncbi.nlm.nih.gov/pmc/articles/PMC3745799/

24. Dekio I, McDowell A, Sakamoto M, Tomida S, Ohkuma M. Proposal of new combination, Cutibacterium acnes subsp. elongatum comb. nov., and emended descriptions of the genus Cutibacterium, Cutibacterium acnes subsp. acnes and Cutibacterium acnes subsp. defendens. International Journal of Systematic and Evolutionary Microbiology. 2019 Apr 1;69(4):1087–92.

25. Borrel V, Gannesen AV, Barreau M, Gaviard C, Duclairoir-Poc C, Hardouin J, et al. Adaptation of acneic and non acneic strains of Cutibacterium acnes to sebum-like environment. MicrobiologyOpen. 2019 Apr 4;8(9).

26. Yu Y, Champer J, Agak GW, Kao S, Modlin RL, Kim J. Different Propionibacterium acnes Phylotypes Induce Distinct Immune Responses and Express Unique Surface and Secreted Proteomes. Journal of Investigative Dermatology. 2016 Nov;136(11):2221–8.

27. Allhorn M, Arve S, Brüggemann H, Lood R. A novel enzyme with antioxidant capacity produced by the ubiquitous skin colonizer Propionibacterium acnes. Scientific Reports. 2016 Nov 2;6(1).

28. Platsidaki E, Dessinioti C. Recent advances in understanding Propionibacterium acnes (Cutibacterium acnes) in acne. F1000Research [Internet]. 2018 Dec 19;7:1953. Available from: https://www.ncbi.nlm.nih.gov/pmc/articles/PMC6305227/

29. Balducci E, Papi F, Capialbi DE, Del Bino L. Polysaccharides' Structures and Functions in Biofilm Architecture of Antimicrobial-Resistant (AMR) Pathogens. International Journal of Molecular Sciences. 2023 Feb 17;24(4):4030.

30. Fong JNC, Yildiz FH. Biofilm Matrix Proteins. Microbiology Spectrum. 2015 Apr 1;3(2).

31. Gannesen AV, Zdorovenko EL, Botchkova EA, Hardouin J, Massier S, Kopitsyn DS, et al. Composition of the Biofilm Matrix of Cutibacterium acnes Acneic Strain RT5. Frontiers in Microbiology. 2019 Jun 21;10.

32. Panlilio H, Rice CV. The role of extracellular DNA in the formation, architecture, stability, and treatment of bacterial biofilms. Biotechnology and bioengineering [Internet]. 2021 Jun 1 [cited 2022 Oct 10];118(6):2129–41. Available from: https://www.ncbi.nlm.nih.gov/pmc/articles/PMC8667714/

33. Alkhawaja E, Hammadi S, Abdelmalek M, Mahasneh N, Alkhawaja B, Abdelmalek SM. Antibiotic resistant Cutibacterium acnes among acne patients in Jordan: a cross sectional study. BMC Dermatology. 2020 Nov 17;20(1).

34. Peeters E, Nelis HJ, Coenye T. Comparison of multiple methods for quantification of microbial biofilms grown in microtiter plates. Journal of Microbiological Methods. 2008 Feb;72(2):157–65.

35. Wilson C, Lukowicz R, Merchant S, Valquier-Flynn H, Caballero J, Sandoval J, et al. Quantitative and Qualitative Assessment Methods for Biofilm Growth: A Mini-review. Research & reviews Journal of engineering and technology [Internet]. 2017;6(4):http://www.rroij.com/open-access/quantitative-and-qualitative-assessment-methods-for-biofilm-growth-a-minireview-.pdf. Available from: https://www.ncbi.nlm.nih.gov/pmc/articles/PMC6133255/

36. Absorbance Measurements | BMG LABTECH [Internet]. www.bmglabtech.com. Available from: https://www.bmglabtech.com/en/absorbance/#:~:text=2%3A%20Absorbance%20is%20measured%20by

37. Uzarski JS, DiVito MD, Wertheim JA, Miller WM. Essential design considerations for the resazurin reduction assay to noninvasively quantify cell expansion within perfused extracellular matrix scaffolds. Biomaterials. 2017 Jun;129:163–75.

38. Kuete V, Karaosmanoğlu O, Sivas H. Anticancer Activities of African Medicinal Spices and Vegetables. Medicinal Spices and Vegetables from Africa [Internet]. 2017;271–97. Available from: https://www.sciencedirect.com/science/article/pii/B9780128092866000108

39. Resazurin Cell Viability Assay | Creative Bioarray [Internet]. www.creative-bioarray.com. Available from: https://www.creative-bioarray.com/support/resazurin-cell-viability-assay.htm

40. Corvec S. Clinical and Biological Features of Cutibacterium (Formerly Propionibacterium) avidum, an Underrecognized Microorganism. Clinical Microbiology Reviews. 2018 May 30;31(3).

41. Koizumi J, Nakase K, Hayashi N, Nasu Y, Hirai Y, Nakaminami H. Multidrug-resistant Cutibacterium avidum isolated from patients with acne vulgaris and other infections. Journal of Global Antimicrobial Resistance. 2022 Jan;

42. Saggu SK, Jha G, Mishra PC. Enzymatic Degradation of Biofilm by Metalloprotease From Microbacterium sp. SKS10. Frontiers in Bioengineering and Biotechnology. 2019 Aug 7;7.

43. Gilan I, Sivan A. Effect of proteases on biofilm formation of the plastic-degrading actinomyceteRhodococcus ruberC208. FEMS Microbiology Letters. 2013 Mar 18;342(1):18–23.

44. Trevisol TC, Henriques RO, Souza AJA, Furigo A. An overview of the use of proteolytic enzymes as exfoliating agents. Journal of Cosmetic Dermatology. 2021 Dec 12;21(8):3300–7.

45. Fang JY, Chou WL, Lin CF, Sung CT, Alalaiwe A, Yang SC. Facile Biofilm Penetration of Cationic Liposomes Loaded with DNase I/Proteinase K to Eradicate Cutibacterium acnes for Treating Cutaneous and Catheter Infections. International Journal of Nanomedicine. 2021 Dec 1;Volume 16:8121–38.

46. Bronnec V, Eilers H, Jahns AC, Omer H, Alexeyev OA. Propionibacterium (Cutibacterium) granulosum Extracellular DNase BmdE Targeting Propionibacterium (Cutibacterium) acnes Biofilm Matrix, a Novel Inter-Species Competition Mechanism. Frontiers in Cellular and Infection Microbiology. 2022 Jan 13;11.

47. Ferraboschi P, Ciceri S, Grisenti P. Applications of Lysozyme, an Innate Immune Defense Factor, as an Alternative Antibiotic. Antibiotics [Internet]. 2021 Dec 14;10(12):1534. Available from: https://www.ncbi.nlm.nih.gov/pmc/articles/PMC8698798/

48. Farfán J, Gonzalez JM, Vives M. The immunomodulatory potential of phage therapy to treat acne: a review on bacterial lysis and immunomodulation. PeerJ. 2022 Jul 25;10:e13553.

49. Cebrián R, Arévalo S, Rubiño S, Arias-Santiago S, Rojo MD, Montalbán-López M, et al. Control of Propionibacterium acnes by natural antimicrobial substances: Role of the

bacteriocin AS-48 and lysozyme. Scientific Reports [Internet]. 2018 Aug 6;8(1):11766. Available from: https://www.nature.com/articles/s41598-018-29580-7

50. Malloci I. EU Cosmetic Products Regulation: An Essential Guide [Internet]. Compliance Gate. 2024 [cited 2024 May 30]. Available from: https://www.compliancegate.com/cosmetics-regulations-european-union/#Regulation_EC_No_12232009_on_Cosmetics_Products

51. De Canha MN, Thipe VC, Katti KV, Mandiwana V, Kalombo ML, Ray SS, et al. The Activity of Gold Nanoparticles Synthesized Using Helichrysum odoratissimum Against Cutibacterium acnes Biofilms. Frontiers in Cell and Developmental Biology. 2021 Sep 13;9.

52. Coenye T, Peeters E, Nelis HJ. Biofilm formation by Propionibacterium acnes is associated with increased resistance to antimicrobial agents and increased production of putative virulence factors. Research in Microbiology. 2007 May;158(4):386–92.

53. O'Neill AM, Cavagnero KJ, Seidman JS, Zaramela L, Chen Y, Li F, et al. Genetic and Functional Analyses of Cutibacterium Acnes Isolates Reveal the Association of a Linear Plasmid with Skin Inflammation. Journal of Investigative Dermatology [Internet]. 2024 Jan 1;144(1):116-124.e4. Available from: https://www.sciencedirect.com/science/article/pii/S0022202X23024156

Appendix

Appendix A

Risk assessment

Risk Assessment of Laboratory Work with Chemicals (AFS 2011:19)[1] (LBE)[2] (MSBFS 2020:1)[3]

Department/Division	Division of Biotechnology
Operation/Activity	Investigations on *C. acnes* biofilms

The operation includes handling of the following chemicals, mixtures and solutions

	Chemical/Mixture/Solution	CAS No.	Approx. amount	Indications of danger
1	Liquid protease preparations	7732-18-5, 84961-57-9,	< 1g	Not hazardous
2	Liquid nuclease	9025-65-4	< 1g	Food grade product
3	Lysozyme	12650-88-3	< 1g	Food grade product
4	Crystal violet	548-62-9	< 5g	Carcinogenicity (2) Aquatic toxicity (1)
5	Resazurin	62758-13-8	< 15mL	Serious eye damage/eye irritation (2)
6	Acetic acid	64-19-7	< 500g	Skin irritation (1) Serious eye damage (1)
7	Ethanol	64-17-5	< 200g	Causes serious eye damage Highly flammable liquid and vapour
8	Methanol	67-56-1	< 500g	Toxic if inhaled
9	Carbenicillin	4800-94-6	< 1g	symptoms or breathing difficulties if
10	TRIS	77-86-1	10g	Not hazardous
11	HCl	7647-01-0	< 10mL	Causes severe skin burn and eye damage
12	BHI	na	200g	Not hazardous
13	Glucose	50-99-7	< 1g	Not hazardous
14	Sodium Chloride	7647-14-5	50g	Not hazardous
15	Deionized water	7732-18-5	-	Not hazardous
16	PBS	7558-79-4	1kg	Not hazardous
17	DPBS	7558-79-4	500g	Not hazardous
18	Glycerin	56-81-5	200g	Not hazardous
19	Xanthan	11138-66-2	< 1g	Not hazardous
20	Xylitol	87-99-0	15g	Not hazardous
21	Magnesium Chloride	7791-18-6	< 1g	Not hazardous
22	Penthylen Glycol	5343-92-0	5g	May irritate skin and eyes
23	Niacinamide	98-92-0	10g	Can cause serios eye irritation (2)
24	Caprylic Capric triglyceride	73398-61-5	20g	Not hazardous
25	Cosmetic surfactant mix	8030-76-0, 7732-18-5	5g	Not hazardous

Identification of separate operations/activities that may involve the risk of accident or risk to health

	Operation/Activity	Risk/Problem	Consequence	Probability	Assessed risk	Risk-reducing measures
1	Handling of crystal violet	Exposure to dust and particles	Toxic to aquatic life with long	Possible	Hazardous	Avoid release to the environment, use gloves/protective clothing/eye protection
2	Handling of resazurin	Exposure to splashing and spillage	Eye and skin irritation	Possible	Hazardous	Wash skin thoroughly after handling, use in a well-ventilated area, wear protective gloves
3	Handling of acetic acid	Exposure to splashing and spillage	Severe skin burns and eye damage	Possible	Hazardous	Keep away from heat, wear protective gloves, rinse with water if on skin
4	Handling of methanol	Exposure to splashing and spillage	Toxic if swallowed, in contact with skin or if inhaled.	Possible	Hazardous	Perform in fume hood, use gloves
5	Handling of ethanol	Exposure to splashing and spillage	Eye irritation	Possible	Moderately Hazardous	Keep away from heat, wear protective gloves, rinse with water if on skin
6	Handling of HCl	Exposure to splashing and spillage	Skin burn and eye damage, Respiratory irritation	Possible	Very Hazardous	Use gloves, absorb spillage
7	Handling of penthylen glycol	Exposure to splashing and spillage	Eye and skin irritation	Possible	Hazardous	Wash skin thoroughly after handling, wear protective gloves and eye protection
8	Handling of carbinicillin	Exposure to splashing and spillage	Eye and skin irritation Respiratory irritation	Possible	Hazardous	Avoid breathing vapors, keep contaminated work clothing in the workplace, wear protective gloves, wash with water if on skin
9	Handling of niacinamide	Exposure to dust and particles	Eye irritation	Possible	Moderately Hazardous	Use glasses

	Yes/No	Comments:
Rules for working alone has been observed	☐	
The possibility of evacuation and ventilation/water/power failure has been taken into account	☐	
Environmental issues have been considered	☐	
Special risk assessment for pregnant staff has been done	☐	

Date:	Risk assessment made by:	Risk assessment checked by:
5/31/2024	Name: Mikaela Fransson & Åsa Leide	Name: Adel Abouhma

Appendix B

Measurements and pictures

Biofilm optimization assay

The OD_{600nm} after 24 h of cell cultivation was 0.86. This was diluted to an OD_{600nm} of 0.1 before inoculation.

Table 1. CV absorbance values for 4 h adhesion and 24 h biofilm formation. Mean = 0.2041.

Plate 1	1	2	3	4	5	6	7	8	9	10	11	12
A	0.178	0.2	0.24	0.176	0.186	0.194	0.259	0.181	0.182	0.168	0.147	0.18
B	0.337	0.263	0.19	0.18	0.199	0.251	0.219	0.204	0.216	0.196	0.165	0.212
C	0.305	0.214	0.21	0.212	0.185	0.181	0.201	0.192	0.208	0.194	0.203	0.188
D	0.214	0.22	0.193	0.206	0.175	0.214	0.201	0.17	0.189	0.191	0.19	0.202
E	0.203	0.196	0.186	0.218	0.178	0.192	0.214	0.203	0.226	0.195	0.213	0.209
F	0.216	0.208	0.194	0.189	0.192	0.192	0.224	0.178	0.185	0.177	0.185	0.183
G	0.225	0.177	0.205	0.172	0.165	0.203	0.219	0.155	0.184	0.17	0.159	0.197
H	0.251	0.27	0.226	0.214	0.192	0.296	0.254	0.246	0.224	0.237	0.221	0.193

Table 2. CV absorbance values for 4 h adhesion and 48 h biofilm formation, media was changed in row E-H after 24 h. Mean (A-D) = 0.5082 and mean (E-H) = 1.0554.

Plate 2	1	2	3	4	5	6	7	8	9	10	11	12
A	0.321	0.529	0.319	0.451	0.439	0.431	0.665	0.474	0.614	0.509	0.525	0.493
B	0.414	0.463	0.556	0.455	0.54	0.547	0.497	0.466	0.588	0.552	0.673	0.618
C	0.447	0.534	0.527	0.539	0.507	0.628	0.514	0.503	0.576	0.495	0.542	0.418
D	0.478	0.519	0.519	0.478	0.395	0.573	0.524	0.52	0.544	0.503	0.565	0.405
E	0.984	1.18	1.35	0.675	0.962	1.174	1.067	1.123	1.216	1.3	1.313	1.426
F	1.222	0.921	0.96	1.085	0.972	1.480	0.984	1.037	0.812	0.987	1.014	0.982
G	1.278	0.892	1.329	1.353	0.972	0.992	1.24	1.344	0.922	1.024	1.303	1.049
H	0.527	0.792	0.576	0.929	0.717	1.508	1.155	0.899	1.146	0.88	0.907	0.699

Table 3. CV absorbance values for 4 h adhesion and 72 h biofilm formation, media was changed in row E-H every 24 h. Mean (A-D) = 0.2972 and mean (E-H) = 0.9927.

Plate 3	1	2	3	4	5	6	7	8	9	10	11	12
A	0.191	0.238	0.338	0.281	0.256	0.271	0.3	0.3	0.217	0.203	0.292	0.199
B	0.245	0.301	0.376	0.335	0.327	0.329	0.31	0.376	0.392	0.371	0.327	0.323
C	0.333	0.281	0.268	0.251	0.282	0.289	0.334	0.336	0.308	0.294	0.344	0.288
D	0.284	0.23	0.258	0.232	0.272	0.323	0.318	0.248	0.39	0.369	0.329	0.305
E	0.489	0.442	0.572	0.713	0.699	0.719	0.768	0.629	0.809	0.82	1.067	0.538
F	0.704	0.988	0.806	0.922	1.341	1.56	2.794	1.21	1.255	1.211	0.952	0.943
G	1.293	0.719	0.949	0.631	0.915	2.53	1.212	2.085	0.85	1.309	1.499	1.043
H	0.262	0.525	0.648	0.706	1.014	1.784	0.749	0.912	0.962	1.007	0.589	0.506

Figure 1. Image of a 96-well plate (Plate 3) from a CV assay, showing biofilm formation after an initial 4 h adhesion time followed by 72 h biofilm growth, media was changed in row E-H every 24 h.

Table 4. CV absorbance values for 24 h adhesion and 24 h biofilm formation. Mean (A-H) = 0.4155. Acetic acid used in columns 1-6 and ethanol in columns 7-12. Wells C6 and F6 emptied for CFU calculations.

Plate 4	1	2	3	4	5	6	7	8	9	10	11	12
A	0.281	0.285	0.358	0.308	0.322	0.288	0.563	0.588	0.654	0.56	0.588	0.473
B	0.562	0.43	0.556	0.623	0.453	0.295	0.517	0.307	0.431	0.488	0.428	0.787
C	0.51	0.223	0.252	0.288	0.321	0.079	0.296	0.262	0.486	0.426	0.567	0.56
D	0.59	0.263	0.29	0.277	0.351	0.354	0.295	0.306	0.426	0.409	0.393	0.642
E	0.55	0.224	0.28	0.327	0.316	0.295	0.339	0.351	0.493	0.497	0.535	0.449
F	0.584	0.378	0.342	0.366	0.317	0.084	0.355	0.32	0.496	0.505	0.506	0.528
G	0.525	0.324	0.349	0.302	0.31	0.303	0.323	0.334	0.515	0.462	0.504	0.479
H	0.532	0.473	0.449	0.436	0.379	0.404	0.356	0.354	0.48	0.58	0.578	0.685

Figure 2. Image of a 96-well plate (Plate 4) from a CV assay, showing biofilm formation after an initial 24 h adhesion time followed by 24 h biofilm growth. Wells C6 and F6 emptied for CFU calculations.

Figure 3. Colonization of *C. acnes* after 24 h adhesion and 24 h biofilm formation to calculate CFU.

Table 5. CV absorbance values for 24 h adhesion and 48 h biofilm formation, media was changed in row E-H after 24 h. Mean (A-D) = 0.7848 and mean (E-H) = 0.7430.

Plate 5	1	2	3	4	5	6	7	8	9	10	11	12
A	0.516	0.482	0.352	0.357	0.426	0.4	0.416	0.411	0.456	0.444	0.506	0.443
B	0.799	0.648	0.713	0.711	0.911	0.784	0.67	0.713	0.676	0.518	0.454	0.577
C	0.816	1.114	1.144	1.184	1.233	1.162	0.939	0.925	0.716	0.822	0.722	0.835
D	0.74	0.76	1.358	0.858	1.478	1.209	1.26	0.744	1.232	0.861	1.482	0.694
E	1.145	0.59	0.513	1.131	0.441	0.733	0.574	0.544	0.427	0.394	0.416	0.965
F	1.817	0.67	0.567	0.488	0.766	0.52	0.551	0.533	0.506	0.572	0.492	0.962
G	1.216	1.185	1.645	0.56	0.508	0.47	0.532	0.471	1.018	0.618	0.538	1.356
H	2.253	1.071	0.732	0.636	0.469	0.731	0.843	0.482	0.522	0.498	0.524	0.474

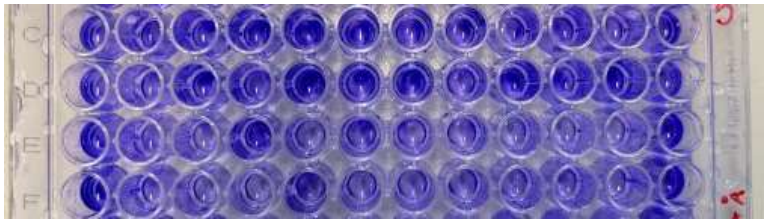

Figure 4. Image of a 96-well plate (Plate 5) from a CV assay, showing biofilm formation after an initial 24 h adhesion time followed by 48 h biofilm growth, media was changed in row E-H after 24 h.

The OD_{600nm} after 24 h of cell cultivation was 2.33. This was diluted to an OD_{600nm} of 0.1 before inoculation.

Table 6. Control plate for *C. avidum* experiment 1 with 4 h adhesion and 24 h biofilm formation. CV absorbance values (columns 1-6), and resazurin absorbance and fluorescence values (columns 7-12). Rows A-B negative control, rows C-D positive control, rows E-F buffer control and rows G-H antimicrobial control.

Plate 6	1	2	3	4	5	6	7	8	9	10	11	12
A	0,129	0,212	0,133	0,149	0,167	0,279	0,248	0,162	0,233	0,21	0,19	0,223
							36432	27389	29698	26044	25065	36703
B	0,194	0,133	0,114	0,121	0,136	0,12	0,258	0,191	0,22	0,185	0,212	0,216
							25261	19071	26240	19036	24084	32369
C	0,301	0,267	0,311	0,262	0,24	0,246	0,306	0,227	0,363	0,398	0,382	0,253
							32997	25594	28558	27942	33441	34623
D	0,3	0,24	0,229	0,264	0,25	0,342	0,237	0,275	0,369	0,22	0,272	0,258
							20434	39265	28333	26364	29718	27823
E	0,224	0,308	0,236	0,182	0,194	0,258	0,185	0,19	0,217	0,192	0,174	0,173
							11711	6059	12510	11732	12826	14443
F	0,316	0,213	0,301	0,276	0,256	0,34	0,275	0,264	0,263	0,265	0,219	0,239
							34915	24130	29917	45155	41466	40990
G	0,874	0,98	0,791	0,55	0,432	0,242	0,145	0,135	0,129	0,115	0,116	0,109
							7632	5278	5155	5661	7508	8324
H	0,132	0,099	0,121	0,327	0,183	0,209	0,123	0,12	0,112	0,11	0,122	0,107
							7137	6279	6535	6057	8020	7446

Table 7. CV absorbance values for *C. avidum* after 4 h adhesion, 24 h biofilm formation, and 24 h treatment with enzymes. The enzyme locations are as follows in decreasing concentrations from top to bottom: Nuclease I (A1:D3), Lysozyme I (A4:D6), Protease I (A7:D9), Protease II (A10:D12), Nuclease II (E1:H3), Protease III (E4:H6), Protease IV (E7:H9), and Anti-acneic peptide (E10:H12).

Plate 7	1	2	3	4	5	6	7	8	9	10	11	12
A	0.176	0.138	0.231	0.707	0.58	0.655	1.479	1.036	1.773	0.308	0.347	0.328
B	0.215	0.237	0.271	2.071	2.106	2.426	0.992	1.266	1.371	0.223	0.252	0.399
C	0.19	0.21	0.273	2.279	2.479	2.23	1.236	1.091	1.063	0.615	0.242	0.431
D	0.169	0.202	0.222	2.474	0.764	1.472	1.162	0.987	1.012	0.287	0.559	0.521
E	0.163	0.159	0.325	0.423	0.456	0.302	1.382	1.403	1.148	0.423	0.676	0.542
F	0.162	0.218	0.206	0.948	0.971	0.869	1.179	0.877	0.977	0.515	0.547	0.511
G	0.191	0.186	0.173	1.249	1.176	1.09	0.66	0.724	0.897	0.747	0.275	0.614
H	0.143	0.204	0.187	1.499	1.719	1.67	0.477	0.461	0.471	0.597	0.589	0.573

Table 8. Resazurin absorbance and fluorescence values for *C. avidum* after 4 h adhesion, 24 h biofilm formation, and 24 h treatment with enzymes. The enzyme locations are as follows in decreasing concentrations from top to bottom: Nuclease I (A1:D3), Lysozyme I (A4:D6), Protease I (A7:D9), Protease II (A10:D12), Nuclease II (E1:H3), Protease III (E4:H6), Protease IV (E7:H9), and Anti-acneic peptide (E10:H12).

Plate 8	1	2	3	4	5	6	7	8	9	10	11	12
A	0.224	0.186	0.231	0.127	0.124	0.123	0.202	0.189	0.168	0.249	0.205	0.229
	10414	13974	16400	9889	12513	17224	8125	7465	7350	10188	11759	10184
B	0.272	0.244	0.226	0.16	0.166	0.162	0.29	0.215	0.219	0.27	0.252	0.194
	12803	13614	14946	25711	28885	28024	9994	7832	6961	13011	12086	16571
C	0.236	0.227	0.204	0.217	0.211	0.152	0.187	0.185	0.181	0.172	0.201	0.208
	12118	15185	15734	29654	47249	21925	6490	7479	7655	11126	12538	10227
D	0.225	0.28	0.229	0.389	0.319	0.517	0.221	0.206	0.177	0.193	0.231	0.247
	14950	17725	16050	34556	45308	43504	7823	7596	8036	11098	13384	10614
E	0.257	0.193	0.199	0.294	0.389	0.346	0.218	0.352	0.436	0.21	0.257	0.191
	13758	10954	13955	5017	6448	5900	1907	803	582	12080	13557	13499
F	0.19	0.182	0.213	0.243	0.245	0.276	0.279	0.21	0.276	0.203	0.209	0.187
	14586	13775	15265	7129	7059	5867	3964	2249	2912	13349	15938	15376
G	0.174	0.164	0.172	0.25	0.245	0.233	0.234	0.207	0.213	0.183	0.187	0.192
	13133	10589	11276	5811	8128	4286	9639	5559	6348	15475	15434	15121
H	0.163	0.171	0.184	0.174	0.189	0.173	0.203	0.154	0.211	0.189	0.191	0.226
	10793	11683	11657	2403	2464	2519	12549	10986	15251	15268	15249	17001

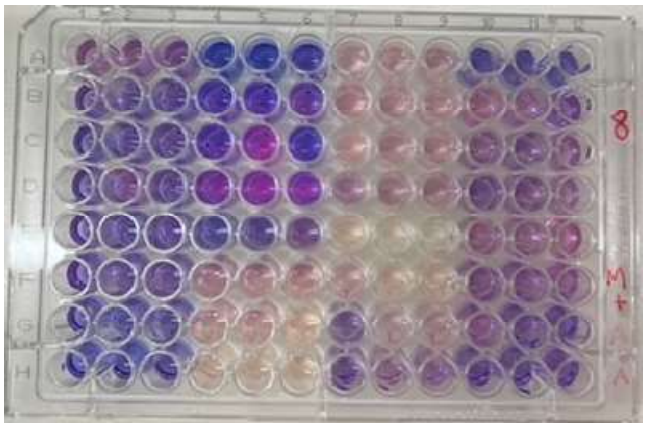

Figure 5. Image of a 96-well plate (Plate 8) from the resazurin assay, showing cell viability after an initial 4 h adhesion time followed by 24 h biofilm growth and 24 h enzyme treatment. The resazurin incubation time was 1 h.

C. avidum Experiment 2

The OD_{600nm} after 24 h of cell cultivation was 1.44. This was diluted to an OD_{600nm} of 0.1 before inoculation.

Table 9. Control plate for *C. avidum* experiment 2 after 24 h adhesion and 24 h biofilm formation. CV absorbance values (columns 1-6), and resazurin absorbance and fluorescence values (columns 7-12). Rows A-B negative control, rows C-D positive control, rows E-F buffer control and rows G-H antimicrobial control.

Plate 1	1	2	3	4	5	6	7	8	9	10	11	12
A	0,085	0,128	0,105	0,197	0,099	0,143	0,083 12554	0,088 13510	0,086 13242	0,087 12919	0,084 13101	0,084 12942
B	0,096	0,161	0,412	0,397	3,553	0,102	0,086 12558	0,098 12945	0,089 12256	0,107 12487	0,086 12381	0,092 14030
C	0,145	0,154	0,141	0,286	0,174	1,499	0,13 45266	0,109 24719	0,112 25437	0,103 17792	0,099 18661	0,093 16556
D	0,174	0,221	0,151	0,169	0,164	0,15	0,107 17731	0,099 15514	0,098 15049	0,094 14454	0,097 13553	0,091 15580
E	0,133	0,172	0,139	0,132	0,153	0,242	0,097 12846	0,094 12925	0,095 14318	0,092 13823	0,092 13265	0,085 12714
F	0,12	0,132	0,182	0,298	0,2	0,156	0,152 26410	0,114 21178	0,118 23441	0,121 22856	0,102 16683	0,106 17876
G	0,111	0,103	0,134	0,737	0,202	0,205	0,103 13824	0,093 12063	0,105 17128	0,102 16004	0,1 16926	0,136 28876
H	0,165	0,098	0,095	0,098	0,115	0,113	0,093 13460	0,093 12538	0,084 11974	0,08 11486	0,08 12817	0,082 12440

Table 10. CV absorbance values for *C. avidum* after 24 h adhesion, 24 h biofilm formation, and 5 h treatment with enzymes. The enzyme locations are as follows in decreasing concentrations from top to bottom: Nuclease I (A1:D3), Lysozyme I (A4:D6), Protease I (A7:D9), Protease II (A10:D12), Nuclease II (E1:H3), Protease III (E4:H6), Protease IV (E7:H9), and Anti-acneic peptide (E10:H12).

Plate 2	1	2	3	4	5	6	7	8	9	10	11	12
A	0,135	0,135	0,137	0,173	0,18	0,209	0,14	0,148	0,157	0,146	0,165	0,236
B	0,161	0,15	0,176	0,236	0,234	0,264	0,141	0,138	0,148	0,16	0,199	0,163
C	0,161	0,158	0,149	0,181	0,175	0,217	0,148	0,146	0,151	0,159	0,171	0,169
D	0,171	0,155	0,139	0,156	0,176	0,214	0,146	0,132	0,13	0,168	0,184	0,175
E	0,15	0,146	0,14	0,152	0,155	0,167	0,144	0,129	0,146	0,163	0,184	0,207
F	0,144	0,156	0,141	0,155	0,156	0,182	0,149	0,143	0,155	0,167	0,18	0,186
G	0,143	0,138	0,151	0,142	0,135	0,138	0,13	0,136	0,161	0,158	0,179	0,173
H	0,136	0,14	0,143	0,136	0,142	0,154	0,128	0,145	0,141	0,175	0,187	0,174

Table 11. Resazurin absorbance and fluorescence values for *C. avidum* after 24 h adhesion, 24 h biofilm formation, and 5 h treatment with enzymes. The enzyme locations are as follows in decreasing concentrations from top to bottom: Nuclease I (A1:D3), Lysozyme I (A4:D6), Protease I (A7:D9), Protease II (A10:D12), Nuclease II (E1:H3), Protease III (E4:H6), Protease IV (E7:H9), and Anti-acneic peptide (E10:H12).

Plate 3	1	2	3	4	5	6	7	8	9	10	11	12
A	0,1	0,112	0,103	0,134	0,151	0,141	0,172	0,162	0,264	0,075	0,087	0,087
	24723	30407	22608	32055	38137	24159	46974	28975	44668	14325	14544	17123
B	0,114	0,114	0,112	0,106	0,1	0,118	0,149	0,112	0,19	0,089	0,098	0,095
	38176	35359	30250	30764	23850	22818	29910	18503	33345	17850	23260	23853
C	0,123	0,122	0,113	0,096	0,098	0,105	0,11	0,13	0,142	0,095	0,094	0,099
	42395	29121	26673	16341	18673	17717	18092	22802	25225	23903	20373	25066
D	0,113	0,107	0,109	0,1	0,119	0,098	0,115	0,098	0,144	0,108	0,113	0,101
	26531	27481	20292	14601	17503	15462	21855	14678	21116	19409	19487	25145
E	0,108	0,107	0,12	0,108	0,112	0,1	0,117	0,101	0,103	0,097	0,099	0,104
	29802	25327	23476	14301	15131	14037	16661	25918	15852	16261	16904	20776
F	0,117	0,121	0,12	0,109	0,121	0,104	0,187	0,137	0,135	0,108	0,12	0,112
	29984	24607	33993	25633	26462	20525	49967	19665	28012	22466	23527	24850
G	0,117	0,112	0,106	0,104	0,106	0,097	0,127	0,11	0,12	0,093	0,125	0,103
	31049	22819	20917	24171	24937	21782	21816	24606	25940	15924	18604	20774
H	0,119	0,106	0,105	0,109	0,104	0,102	0,147	0,137	0,125	0,103	0,101	0,112
	30214	23435	22014	29622	24524	25718	38801	23321	24301	19811	19302	20578

C. acnes Experiment 2

The OD_{600nm} after 24 h of cell cultivation was 2.25. This was diluted to an OD_{600nm} of 0.1 before inoculation.

Table 12. Control plate for *C. acnes* experiment 2 after 4 h adhesion and 44 h biofilm formation. CV absorbance values (columns 1-6), and resazurin absorbance and fluorescence values (columns 7-12). Rows A-B negative control, rows C-D positive control, rows E-F buffer control and rows G-H antimicrobial control.

Plate 4	1	2	3	4	5	6	7	8	9	10	11	12
A	0,452	0,116	0,141	0,164	0,195	0,154	0,089	0,127	0,108	0,099	0,091	0,099
							4453	12987	5741	7882	5809	5119
B	0,266	0,193	0,256	0,265	0,154	0,173	0,105	0,097	0,1	0,091	0,123	0,138
							6700	8080	9301	5345	12474	14955
C	0,392	0,36	0,457	0,351	0,406	0,478	0,158	0,177	0,154	0,144	0,128	0,2
							32104	23445	26656	25686	22316	34664
D	1,597	0,338	0,374	0,314	0,602	0,659	0,124	0,127	0,142	0,123	0,135	0,172
							22228	15387	27625	22031	26370	35836
E	0,456	0,535	0,475	0,391	0,816	0,614	0,129	0,204	0,127	0,165	0,197	0,301
							19415	25242	19319	28062	35798	46097
F	0,182	0,138	0,164	0,204	0,35	0,291	0,088	0,093	0,094	0,091	0,103	0,127
							6092	7614	7544	7032	12231	15016
G	0,481	0,271	0,311	0,191	0,285	0,346	0,108	0,122	0,103	0,106	0,135	0,151
							19502	17292	10743	18342	27948	34119
H	0,206	0,352	0,163	0,171	0,221	0,185	0,107	0,093	0,116	0,102	0,135	0,144
							9319	5321	9508	6469	11124	13407

Table 13. CV absorbance values for *C. acnes* after 4 h adhesion, 44 h biofilm formation, and 4 h treatment with enzymes. The enzyme locations are as follows in decreasing concentrations from top to bottom: Nuclease I (A1:D3), Lysozyme I (A4:D6), Protease I (A7:D9), Protease II (A10:D12), Nuclease II (E1:H3), Protease III (E4:H6), Protease IV (E7:H9), and Anti-acneic peptide (E10:H12).

Plate 5	1	2	3	4	5	6	7	8	9	10	11	12
A	0,135	0,15	0,145	0,308	0,311	0,221	0,128	0,118	0,135	0,111	0,135	0,141
B	0,141	0,127	0,157	0,235	0,247	0,205	0,146	0,135	0,131	0,141	0,148	0,138
C	0,138	0,141	0,131	0,165	0,171	0,153	0,111	0,13	0,129	0,143	0,141	0,135
D	0,143	0,148	0,139	0,144	0,153	0,156	0,121	0,113	0,137	0,122	0,148	0,147
E	0,124	0,14	0,117	0,129	0,158	0,158	0,129	0,11	0,128	0,196	0,191	0,211
F	0,135	0,112	0,122	0,117	0,143	0,12	0,133	0,118	0,123	0,238	0,237	0,21
G	0,13	0,129	0,121	0,117	0,136	0,121	0,134	0,139	0,151	0,163	0,194	0,161
H	0,179	0,135	0,129	0,141	0,142	0,124	0,117	0,145	0,126	0,204	0,177	0,163

Table 14. Resazurin absorbance and fluorescence values for *C. acnes* after 4 h adhesion, 44 h biofilm formation, and 4 h treatment with enzymes. The enzyme locations are as follows in decreasing concentrations from top to bottom: Nuclease I (A1:D3), Lysozyme I (A4:D6), Protease I (A7:D9), Protease II (A10:D12), Nuclease II (E1:H3), Protease III (E4:H6), Protease IV (E7:H9), and Anti-acneic peptide (E10:H12).

Plate 6	1	2	3	4	5	6	7	8	9	10	11	12
A	0,086	0,085	0,085	0,152	0,152	0,112	0,099	0,102	0,101	0,083	0,099	0,08
	8275	7474	8359	47136	38152	22633	9590	11313	16382	12115	31482	9197
B	0,086	0,082	0,084	0,103	0,111	0,101	0,096	0,103	0,102	0,102	0,09	0,087
	9396	6440	6575	24613	22093	17132	11147	13045	19169	19759	16886	18260
C	0,086	0,085	0,088	0,09	0,094	0,088	0,099	0,106	0,099	0,11	0,105	0,098
	9743	8135	11158	9313	11095	11079	10179	13081	11398	24736	27367	26210
D	0,081	0,082	0,085	0,086	0,085	0,089	0,093	0,094	0,092	0,09	0,098	0,139
	6309	6326	6530	8979	7049	11374	7168	9463	7283	15367	19837	35178
E	0,083	0,082	0,079	0,093	0,103	0,103	0,099	0,097	0,092	0,096	0,093	0,123
	7203	6668	6700	7033	8537	10480	7767	8585	7535	12844	14768	28443
F	0,094	0,078	0,083	0,101	0,114	0,106	0,104	0,106	0,099	0,098	0,088	0,107
	7286	5695	7281	6649	11873	6446	8115	9373	10770	9638	8929	11301
G	0,088	0,084	0,086	0,094	0,11	0,087	0,123	0,114	0,106	0,099	0,1	0,128
	10059	7213	8178	7694	10216	7714	13328	13182	10503	17872	19653	23905
H	0,086	0,082	0,093	0,11	0,103	0,101	0,114	0,106	0,116	0,095	0,089	0,1
	6767	5981	7928	8999	10007	9552	9032	9098	9099	8868	10506	13152

Table 15. Control plate for *C. acnes* experiment 2 after 24 h adhesion and 24 h biofilm formation. CV absorbance values (columns 1-6), and resazurin absorbance and fluorescence values (columns 7-12). Rows A-B negative control, rows C-D positive control, rows E-F buffer control and rows G-H antimicrobial control.

Plate 7	1	2	3	4	5	6	7	8	9	10	11	12
A	0,158	0,199	0,15	0,228	0,297	0,25	0,11	0,125	0,117	0,119	0,117	0,127
							14706	11808	13238	11356	17862	17643
B	0,223	0,179	0,159	0,224	0,181	0,307	0,105	0,102	0,118	0,113	0,112	0,153
							11160	9768	11960	12701	13259	15058
C	1,714	0,849	1,03	1,003	1,083	1,655	0,264	0,227	0,265	0,283	0,218	0,354
							35362	32736	37895	35942	42102	49477
D	1,226	1,109	0,87	0,813	1,495	1,326	0,186	0,234	0,26	0,23	0,235	0,205
							34832	38021	34262	35147	39294	48899
E	1,466	1,02	0,901	1,017	1,147	1,248	0,245	0,369	0,356	0,316	0,299	0,198
							36736	44109	45850	45186	34765	27046
F	0,368	0,321	0,224	0,222	0,25	0,218	0,112	0,101	0,114	0,107	0,116	0,116
							9198	8556	13113	9484	12367	14051
G	0,313	0,4	0,219	0,198	0,296	0,276	0,127	0,125	0,123	0,153	0,154	0,159
							24604	17488	22833	36963	28880	37196
H	0,311	0,392	0,219	0,232	0,318	0,307	0,126	0,146	0,14	0,145	0,176	0,149
							13347	15226	14518	17572	17053	20858

Table 16. CV absorbance values for *C. acnes* after 24 h adhesion, 24 h biofilm formation, and 4 h treatment with enzymes. The enzyme locations are as follows in decreasing concentrations from top to bottom: Nuclease I (A1:D3), Lysozyme I (A4:D6), Protease I (A7:D9), Protease II (A10:D12), Nuclease II (E1:H3), Protease III (E4:H6), Protease IV (E7:H9), and Anti-acneic peptide (E10:H12).

Plate 8	1	2	3	4	5	6	7	8	9	10	11	12
A	0,105	0,109	0,108	0,605	0,707	0,922	0,11	0,112	0,137	0,414	0,338	0,752
B	0,107	0,104	0,104	0,448	0,493	0,549	0,157	0,124	0,203	0,176	0,148	0,158
C	0,171	0,128	0,153	0,28	0,24	0,327	0,181	0,143	0,195	0,199	0,166	0,185
D	0,115	0,123	0,162	0,237	0,22	0,237	0,135	0,141	0,159	0,179	0,152	0,148
E	0,101	0,103	0,11	0,108	0,104	0,143	0,113	0,106	0,129	0,34	0,32	0,382
F	0,107	0,107	0,108	0,162	0,161	0,149	0,154	0,132	0,135	0,283	0,252	0,268
G	0,113	0,103	0,122	0,122	0,134	0,155	0,108	0,125	0,139	0,189	0,223	0,204
H	0,102	0,106	0,114	0,11	0,12	0,131	0,116	0,129	0,126	0,276	0,234	0,239

Table 17. Resazurin absorbance and fluorescence values for *C. acnes* after 24 h adhesion, 24 h biofilm formation, and 4 h treatment with enzymes. The enzyme locations are as follows in decreasing concentrations from top to bottom: Nuclease I (A1:D3), Lysozyme I (A4:D6), Protease I (A7:D9), Protease II (A10:D12), Nuclease II (E1:H3), Protease III (E4:H6), Protease IV (E7:H9), and Anti-acneic peptide (E10:H12).

Plate 9	1	2	3	4	5	6	7	8	9	10	11	12
A	0,087	0,092	0,088	0,301	0,365	0,429	0,099	0,101	0,109	0,256	0,206	0,237
	4440	5614	5686	34713	31959	32052	5603	5447	5626	41029	33116	45324
B	0,094	0,094	0,089	0,29	0,299	0,325	0,1	0,097	0,095	0,116	0,137	0,125
	5506	4868	3741	26648	23469	25527	4504	4101	3793	17026	24793	20130
C	0,105	0,1	0,093	0,153	0,175	0,15	0,1	0,104	0,103	0,128	0,125	0,124
	5727	4453	5437	7799	7786	9142	4688	4772	4996	19162	16697	18887
D	0,096	0,095	0,089	0,112	0,12	0,121	0,101	0,108	0,109	0,13	0,141	0,134
	3991	4562	3721	5006	5425	5425	4043	5406	5014	15341	22878	18395
E	0,096	0,092	0,09	0,102	0,11	0,121	0,108	0,106	0,111	0,196	0,157	0,179
	4028	3808	4056	3907	4191	5023	4901	3930	5367	26964	21234	31129
F	0,096	0,1	0,097	0,111	0,103	0,121	0,122	0,122	0,112	0,143	0,163	0,134
	4759	4447	4576	4206	3933	7104	8022	5610	4566	10736	19728	13856
G	0,114	0,107	0,098	0,124	0,112	0,133	0,117	0,115	0,116	0,141	0,151	0,148
	5908	4680	4940	6330	6653	10648	4696	6708	5104	12113	15429	15307
H	0,124	0,113	0,113	0,124	0,153	0,228	0,129	0,134	0,126	0,156	0,146	0,134
	8214	5706	5920	7221	7792	19136	6353	5734	6693	13987	11817	14231

Table 18. Control plate for *C. acnes* experiment 2 after 24 h adhesion and 48 h biofilm formation. CV absorbance values in all columns, where rows A-B are negative control, rows C-D positive control, rows E-F buffer control and rows G-H antimicrobial control.

Plate 10	1	2	3	4	5	6	7	8	9	10	11	12
A	0,406	0,169	0,282	0,175	0,23	0,134	0,14	0,234	0,146	0,177	0,18	0,123
B	0,256	0,318	0,223	0,256	0,188	0,334	0,263	0,274	0,14	0,174	0,138	0,145
C	1,08	0,77	0,913	0,845	1,185	0,67	0,852	0,495	0,533	0,641	0,442	0,516
D	1,101	0,871	0,727	0,489	0,567	0,566	0,575	0,514	0,5	0,449	0,416	0,492
E	1,013	0,692	0,765	0,546	0,77	0,623	0,848	0,442	0,733	0,559	0,61	0,483
F	0,991	0,811	0,593	0,818	0,682	0,925	0,566	0,483	0,442	0,43	0,493	0,427
G	0,802	0,916	1,139	0,858	0,788	0,775	0,903	0,555	0,595	0,738	0,613	0,495
H	0,711	0,938	1,139	1,037	1,329	1,135	0,967	0,772	0,495	0,532	0,738	1,266

Table 19. CV absorbance values for *C. acnes* after 24 h adhesion, 48 h biofilm formation, and 4 h treatment with enzymes. The enzyme locations are as follows in decreasing concentrations from top to bottom: Nuclease I (A1:D3), Lysozyme I (A4:D6), Protease I (A7:D9), Protease II (A10:D12), Nuclease II (E1:H3), Protease III (E4:H6), Protease IV (E7:H9), and Anti-acneic peptide (E10:H12).

Plate 11	1	2	3	4	5	6	7	8	9	10	11	12
A	0,566	0,577	0,934	0,753	0,646	0,663	0,887	0,641	0,662	0,649	0,66	0,51
B	0,977	0,584	0,792	0,704	0,544	0,69	0,761	0,595	0,591	0,6	0,853	0,585
C	1,118	0,655	1,022	0,59	0,871	0,626	0,636	0,651	0,78	0,458	0,446	0,592
D	1,157	0,585	0,515	0,499	0,501	0,507	0,569	0,514	0,58	0,606	0,718	0,767
E	0,353	0,77	0,784	0,6	0,545	0,61	0,715	0,593	0,781	0,773	0,768	0,502
F	0,804	0,443	0,806	0,556	0,493	0,37	0,454	0,361	0,489	0,395	0,492	0,471
G	1,299	0,85	1,073	1,022	0,953	0,614	0,781	0,697	0,74	0,641	0,672	0,484
H	1,463	0,727	1,15	1,432	1,07	1,136	1,211	1,015	0,958	1,053	0,814	0,825

Table 20. Resazurin absorbance and fluorescence values for *C. acnes* after 24 h adhesion, 48 h biofilm formation, and 4 h treatment with enzymes. The enzyme locations are as follows in decreasing concentrations from top to bottom: Nuclease I (A1:D3), Lysozyme I (A4:D6), Protease I (A7:D9), Protease II (A10:D12), Nuclease II (E1:H3), Protease III (E4:H6), Protease IV (E7:H9), and Anti-acneic peptide (E10:H12).

Plate 12	1	2	3	4	5	6	7	8	9	10	11	12
A	0,383	0,607	0,454	0,681	0,708	0,835	0,622	0,982	0,514	0,504	0,797	0,554
B	0,443	0,524	0,662	0,419	0,567	0,833	0,574	0,908	0,837	0,754	1,024	0,984
C	0,405	0,706	0,561	0,721	0,482	0,719	0,626	0,62	0,464	0,38	0,634	0,454
D	0,614	0,525	0,657	0,621	0,781	0,752	0,573	0,65	0,48	0,714	0,737	0,731
E	0,589	0,508	0,477	0,66	0,806	0,645	0,556	0,883	0,495	0,683	0,791	0,832
F	0,679	0,62	0,61	0,629	0,948	0,534	0,724	0,757	0,724	0,992	0,758	0,58
G	0,69	0,749	1,032	0,865	0,971	0,851	0,984	0,932	0,882	1,078	1,132	0,91
H	0,789	0,706	0,672	0,522	0,984	0,844	1,099	0,906	0,86	1,042	1,056	0,779

The OD_{600nm} after 24 h of cell cultivation was 1.24. This was diluted to an OD_{600nm} of 0.1 before inoculation.

Table 21. Resazurin values measuread after 20 min of incubation at two different wavelengths for absorption (570 nm and 600 nm) and fluorescence (excitation at 540 nm and emission at 590 nm). Measurements were taken after 24 h adhesion, 48 h of biofilm formation, and 4 h of enzyme treatment. The enzyme locations, in decreasing concentrations from top to bottom, are as follows: Nuclease I (A1:H3), Nuclease II (A4:H6), Lysozyme I (A7:H9), and a positive control/blank (A10:H12).

Plate 1	1	2	3	4	5	6	7	8	9	10	11	12	
A	0.73	0.749	0.819	0.7	0.757	0.732	0.573	0.711	0.591	0.735	0.747	0.772	600
	0.621	0.629	0.695	0.662	0.66	0.666	0.581	0.711	0.588	0.646	0.627	0.688	570
	4742	4247	4463	8739	5995	7565	6451	7407	6740	5741	3812	5667	540,590
B	0.791	0.777	0.826	0.786	0.829	0.788	0.72	0.754	0.747	0.798	0.805	0.792	600
	0.655	0.623	0.659	0.689	0.688	0.645	0.622	0.613	0.592	0.63	0.634	0.623	570
	4711	3369	3037	5644	4313	3844	5273	4112	3367	3123	3112	3219	540,590
C	0.814	0.776	0.837	0.741	0.803	0.785	0.714	0.726	0.757	0.79	0.789	0.783	600
	0.677	0.655	0.682	0.614	0.677	0.652	0.583	0.595	0.595	0.621	0.634	0.683	570
	4881	5494	3609	4057	4375	4245	3847	3881	3132	2880	3292	5431	540,590
D	0.78	0.783	0.809	0.758	0.801	0.79	0.764	0.703	0.744	0.808	0.801	0.763	600
	0.639	0.623	0.638	0.611	0.664	0.675	0.586	0.618	0.603	0.677	0.653	0.598	570
	4160	3707	3113	3312	3854	4807	2522	4493	3071	3726	3195	2874	540,590
E	0.795	0.795	0.781	0.762	0.792	0.796	0.764	0.766	0.778	0.822	0.799	0.735	600
	0.631	0.616	0.62	0.603	0.616	0.614	0.588	0.591	0.605	0.658	0.637	0.649	570
	3335	2987	3958	3122	2848	2737	2873	2743	2626	2995	3037	5032	540,590
F	0.802	0.802	0.808	0.79	0.845	0.873	0.767	0.758	0.771	0.783	0.794	0.762	600
	0.622	0.631	0.621	0.615	0.703	0.716	0.608	0.599	0.603	0.74	0.637	0.688	570
	3302	3012	2867	3036	4523	3715	3355	3006	2724	7997	3204	6886	540,590
G	0.795	0.805	0.802	0.774	0.858	0.833	0.78	0.778	0.775	0.801	0.819	0.86	600
	0.617	0.616	0.613	0.61	0.671	0.663	0.605	0.602	0.597	0.674	0.637	0.689	570
	3150	2763	2730	3211	3092	3574	2900	2985	2610	4610	2866	3417	540,590
H	0.819	0.798	0.808	0.771	0.816	0.814	0.763	0.717	0.761	0.706	0.791	0.778	600
	0.645	0.627	0.63	0.626	0.655	0.63	0.649	0.652	0.61	0.646	0.616	0.698	570
	3287	2960	3176	3319	3301	2795	4960	6439	3167	6905	2711	6773	540,590

Table 22. Resazurin values measuread after 60 min of incubation at two different wavelengths for absorption (570 nm and 600 nm) and fluorescence (excitation at 540 nm and emission at 590 nm). Measurements were taken after 24 h adhesion, 48 h of biofilm formation, and 4 h of enzyme treatment. The enzyme locations, in decreasing concentrations from top to bottom, are as follows: Nuclease I (A1:H3), Nuclease II (A4:H6), Lysozyme I (A7:H9), and a positive control/blank (A10:H12).

Plate 1	1	2	3	4	5	6	7	8	9	10	11	12	
A	0.158	0.193	0.276	0.317	0.397	0.443	0.224	0.203	0.207	0.419	0.41	0.437	600
	0.27	0.305	0.363	0.417	0.491	0.555	0.303	0.292	0.292	0.46	0.426	0.496	570
	1023	1368	2504	6613	6140	8900	3264	3699	3045	6627	3764	7049	540,590
B	0.166	0.191	0.393	0.328	0.56	0.466	0.223	0.237	0.302	0.26	0.528	0.646	600
	0.275	0.295	0.407	0.397	0.554	0.474	0.307	0.315	0.341	0.339	0.486	0.551	570
	1041	898	1927	5729	6408	4351	2501	2395	2120	1307	2989	3832	540,590
C	0.178	0.219	0.234	0.28	0.43	0.432	0.362	0.317	0.418	0.46	0.567	0.52	600
	0.291	0.314	0.326	0.347	0.457	0.457	0.399	0.373	0.422	0.445	0.519	0.542	570
	1015	2008	1163	2524	4936	4293	3357	2845	2739	2510	3894	7327	540,590
D	0.15	0.217	0.384	0.233	0.509	0.5	0.353	0.25	0.402	0.389	0.508	0.427	600
	0.269	0.307	0.395	0.315	0.501	0.518	0.371	0.344	0.413	0.428	0.486	0.417	570
	633	1598	1903	1300	4657	6356	1268	2999	2737	3009	3180	2371	540,590
E	0.15	0.187	0.292	0.503	0.384	0.593	0.473	0.442	0.487	0.539	0.486	0.351	600
	0.271	0.291	0.345	0.462	0.391	0.506	0.438	0.423	0.444	0.499	0.465	0.404	570
	503	757	2413	3141	1636	2765	2428	2102	2079	2797	2686	4464	540,590
F	0.183	0.215	0.383	0.574	0.424	0.299	0.281	0.536	0.428	0.497	0.468	0.417	600
	0.287	0.313	0.392	0.499	0.456	0.379	0.347	0.491	0.417	0.588	0.462	0.478	570
	765	828	1551	3174	4023	1952	1825	3380	2024	11984	3288	8133	540,590
G	0.175	0.242	0.199	0.366	0.54	0.581	0.451	0.281	0.501	0.394	0.533	0.494	600
	0.284	0.318	0.297	0.383	0.492	0.526	0.432	0.337	0.448	0.425	0.484	0.474	570
	597	832	614	2241	2714	4271	2374	1482	1976	4164	2543	3043	540,590
H	0.186	0.241	0.303	0.23	0.215	0.257	0.349	0.286	0.242	0.231	0.291	0.263	600
	0.297	0.33	0.354	0.314	0.315	0.329	0.401	0.36	0.321	0.3	0.347	0.336	570
	593	861	1323	1263	1071	922	4029	3670	1405	3296	1175	3367	540,590

Table 23. CV absorbance values for *C. acnes* after 4 h adhesion, 44 h biofilm formation, and 4 h treatment with enzymes. Measurements were made at wavelength 590 nm. The enzyme locations are as follows in decreasing concentrations from top to bottom: Nuclease I (A1:H3), Nuclease II (A4:H6), Lysozyme I (A7:H9), and a positive control/blank (A10:H12).

Plate 2	1	2	3	4	5	6	7	8	9	10	11	12
A	0,137	0,132	0,157	0,225	0,22	0,212	0,221	0,32	0,294	0,331	0,197	0,612
B	0,111	0,15	0,134	0,163	0,164	0,142	0,171	0,139	0,147	0,13	0,14	0,108
C	0,122	0,123	0,12	0,131	0,127	0,136	0,183	0,211	0,13	0,112	0,107	0,15
D	0,113	0,146	0,122	0,118	0,115	0,121	0,12	0,117	0,113	0,117	0,105	0,118
E	0,11	0,126	0,116	0,126	0,117	0,105	0,123	0,135	0,136	0,14	0,107	0,132
F	0,101	0,095	0,112	0,123	0,116	0,101	0,134	0,124	0,114	0,147	0,122	0,133
G	0,099	0,116	0,115	0,115	0,171	0,126	0,116	0,129	0,109	0,133	0,105	0,15
H	0,141	0,136	0,133	0,121	0,122	0,129	0,436	0,567	0,196	0,458	0,233	0,766

Table 24. Resazurin values measured after 20 min of incubation at two different wavelengths for absorption (570 nm and 600 nm) and fluorescence (excitation at 540 nm and emission at 590 nm). Measurements were taken after 24 h adhesion, 48 h of biofilm formation, and 4 h of enzyme treatment. The enzyme locations, in decreasing concentrations from top to bottom, are as follows: Protease IV (A1:H3), Protease III (A4:H6), Protease II (A7:H9), and a positive control/blank (A10:H12).

Plate 3	1	2	3	4	5	6	7	8	9	10	11	12	
A	0.778	0.777	0.751	0.763	0.879	0.756	0.911	0.808	0.894	0.816	0.842	0.77	600
	0.681	0.659	0.625	0.766	0.816	0.8	0.778	0.746	0.751	0.756	0.754	0.737	570
	6160	5348	4800	8086	5835	9617	4797	8628	4105	6698	5400	9074	540,590
B	0.811	0.81	0.659	0.874	0.818	0.822	0.964	0.86	0.877	0.778	0.814	0.797	600
	0.694	0.713	0.629	0.856	0.787	0.749	0.896	0.73	0.755	0.663	0.664	0.688	570
	4659	5283	8904	7714	7641	6934	6523	4745	5119	5145	3590	6246	540,590
C	0.742	0.793	0.777	0.764	0.738	0.806	0.884	0.84	0.867	0.769	0.733	0.932	600
	0.6	0.668	0.642	0.661	0.655	0.779	0.807	0.681	0.728	0.706	0.687	0.886	570
	3786	4101	3933	5559	7114	8614	5847	3464	4178	7187	7792	8471	540,590
D	0.838	0.823	0.753	0.796	0.754	0.848	0.86	0.911	0.815	0.889	0.861	0.928	600
	0.74	0.741	0.699	0.762	0.697	0.773	0.738	0.812	0.697	0.824	0.793	0.902	570
	5283	5448	6238	8037	7648	6805	4519	5420	4645	7166	6988	7485	540,590
E	0.773	0.783	0.798	0.749	0.82	0.809	0.86	0.862	0.841	0.915	0.892	0.896	600
	0.678	0.685	0.708	0.706	0.726	0.79	0.746	0.747	0.698	0.794	0.787	0.801	570
	5339	4945	4884	8229	6760	9221	4816	4710	3639	4014	5037	6521	540,590
F	0.748	0.83	0.759	0.775	0.708	0.822	0.929	0.876	0.87	0.866	1.01	1.063	600
	0.662	0.759	0.684	0.761	0.708	0.78	0.842	0.763	0.743	0.76	0.952	0.993	570
	6084	5761	6805	9119	9288	8504	5499	4526	4731	5081	7412	5497	540,590
G	0.785	0.649	0.775	0.836	0.774	0.809	0.917	0.819	0.745	0.875	0.822	0.909	600
	0.682	0.604	0.658	0.765	0.702	0.817	0.867	0.793	0.718	0.782	0.745	0.84	570
	5383	6319	5855	6344	6310	9196	7256	8423	8706	5121	7412	7140	540,590
H	0.8	0.668	0.759	0.69	0.697	0.749	0.89	0.796	0.753	0.866	0.755	0.827	600
	0.738	0.645	0.673	0.698	0.693	0.734	0.851	0.768	0.766	0.816	0.745	0.798	570
	6943	6961	5732	11804	9983	9333	7178	7371	9623	6561	9239	8428	540,590

Table 25. Resazurin values measuread after 60 min of incubation at two different wavelengths for absorption (570 nm and 600 nm) and fluorescence (excitation at 540 nm and emission at 590 nm). Measurements were taken after 24 h adhesion, 48 h of biofilm formation, and 4 h of enzyme treatment. The enzyme locations, in decreasing concentrations from top to bottom, are as follows: Protease IV (A1:H3), Protease III (A4:H6), Protease II (A7:H9), and a positive control/blank (A10:H12).

Plate 3	1	2	3	4	5	6	7	8	9	10	11	12	
A	0.243	0.271	0.289	0.287	0.336	0.348	0.378	0.473	0.485	0.388	0.334	0.347	600
	0.338	0.354	0.357	0.381	0.441	0.434	0.452	0.591	0.511	0.479	0.427	0.458	570
	4396	3545	3896	3995	3160	5076	3438	12819	4283	7874	4096	9592	540,590
B	0.233	0.329	0.317	0.427	0.358	0.39	0.569	0.6	0.462	0.468	0.405	0.464	600
	0.334	0.425	0.431	0.53	0.463	0.474	0.646	0.61	0.529	0.492	0.434	0.525	570
	1842	3042	10423	4685	5036	5492	10174	7109	5796	5282	2950	7438	540,590
C	0.176	0.257	0.267	0.259	0.333	0.436	0.374	0.362	0.36	0.369	0.337	0.542	600
	0.282	0.359	0.356	0.354	0.418	0.547	0.466	0.421	0.442	0.457	0.422	0.67	570
	944	1496	1978	2223	5035	6045	4274	2405	2993	8202	8069	13661	540,590
D	0.245	0.308	0.349	0.351	0.417	0.5	0.326	0.451	0.535	0.493	0.55	0.495	600
	0.359	0.419	0.458	0.45	0.528	0.61	0.41	0.521	0.561	0.587	0.647	0.604	570
	1404	2049	2965	4057	4877	4974	3232	5339	6208	8542	8184	8204	540,590
E	0.277	0.335	0.322	0.379	0.361	0.515	0.348	0.574	0.373	0.463	0.448	0.517	600
	0.399	0.452	0.432	0.488	0.464	0.622	0.454	0.626	0.444	0.523	0.502	0.58	570
	1470	1748	1987	3692	3554	5913	2301	4710	2124	3135	4014	7321	540,590
F	0.251	0.367	0.373	0.379	0.454	0.36	0.362	0.324	0.438	0.405	0.6	0.519	600
	0.369	0.474	0.473	0.482	0.546	0.459	0.451	0.416	0.494	0.474	0.715	0.612	570
	1378	1811	2766	4175	3896	4827	3063	2687	4185	4287	8484	5466	540,590
G	0.24	0.291	0.287	0.267	0.359	0.344	0.474	0.429	0.373	0.424	0.401	0.609	600
	0.36	0.396	0.393	0.364	0.452	0.453	0.576	0.533	0.461	0.5	0.494	0.702	570
	1050	1720	2166	2516	4276	4555	4987	5125	6178	3683	8579	10599	540,590
H	0.284	0.271	0.364	0.357	0.381	0.303	0.353	0.389	0.259	0.353	0.272	0.417	600
	0.385	0.359	0.479	0.462	0.455	0.39	0.456	0.494	0.352	0.436	0.359	0.544	570
	1341	2011	1725	7626	4117	3759	3397	4708	4208	4167	5070	12510	540,590

Table 26. CV absorbance values for *C. acnes* after 4 h adhesion, 44 h biofilm formation, and 4 h treatment with enzymes. Measurements were made at wavelength 590 nm. The enzyme locations are as follows in decreasing concentrations from top to bottom: Protease IV (A1:H3), Protease III (A4:H6), Protease II (A7:H9), and a positive control/blank (A10:H12).

Plate 4	1	2	3	4	5	6	7	8	9	10	11	12	
A	0.168	0.164	0.177	0.108	0.136	0.123	0.116	0.099	0.121	0.292	0.383	0.535	590
B	0.165	0.129	0.201	0.092	0.103	0.102	0.102	0.088	0.093	0.253	0.133	0.293	590
C	0.127	0.109	0.121	0.085	0.092	0.087	0.101	0.086	0.083	0.235	0.119	0.171	590
D	0.13	0.122	0.093	0.091	0.085	0.081	0.092	0.08	0.077	0.115	0.107	0.136	590
E	0.136	0.131	0.109	0.089	0.08	0.079	0.08	0.083	0.076	0.156	0.131	0.351	590
F	0.176	0.18	0.219	0.089	0.091	0.082	0.16	0.13	0.142	0.265	0.222	0.512	590
G	0.197	0.19	0.148	0.094	0.121	0.093	0.144	0.157	0.279	0.147	0.231	0.126	590
H	0.254	0.234	0.351	0.105	0.186	0.139	0.633	0.548	0.354	0.76	0.389	0.484	590

Table 27. Resazurin values measured after 20 min of incubation at two different wavelengths for absorption (570 nm and 600 nm) and fluorescence (excitation at 540 nm and emission at 590 nm). Measurements were taken after 24 h adhesion, 48 h of biofilm formation, and 4 h of enzyme treatment. The enzyme locations, in decreasing concentrations from top to bottom, are as follows: Protease V (A1:H3), Protease VI (A4:H6), Protease VII (A7:H9), and a positive control/blank (A10:H12).

Plate 5	1	2	3	4	5	6	7	8	9	10	11	12	
A	0.854	0.805	0.879	0.535	0.701	0.649	0.866	0.894	0.91	0.901	0.879	0.86	600
	0.921	0.832	0.897	0.545	0.585	0.58	0.801	0.825	0.88	0.8	0.727	0.726	570
	15007	13129	12533	8979	4966	6483	7985	7987	9798	4826	3773	3693	540,590
B	0.796	0.771	0.834	0.54	0.464	0.535	0.89	0.952	0.88	0.849	0.814	0.775	600
	0.702	0.726	0.77	0.533	0.499	0.567	0.822	0.864	0.788	0.829	0.714	0.755	570
	7130	9885	9169	7704	8736	9548	7909	6363	6938	9789	5741	10426	540,590
C	0.855	0.855	0.836	0.397	0.419	0.485	0.793	0.818	0.835	0.794	0.782	0.86	600
	0.798	0.825	0.775	0.444	0.469	0.491	0.751	0.78	0.782	0.761	0.749	0.798	570
	8326	9507	8329	8522	7296	7820	8969	8859	8664	8500	8566	7209	540,590
D	0.753	0.794	0.824	0.445	0.604	0.604	0.849	0.859	0.829	0.762	0.814	0.839	600
	0.724	0.718	0.726	0.445	0.595	0.585	0.76	0.75	0.754	0.674	0.771	0.738	570
	9000	6409	6322	5385	8440	8228	6441	6264	7222	5651	8914	6091	540,590
E	0.874	0.803	0.805	0.496	0.597	0.697	0.817	0.861	0.803	0.777	0.826	0.914	600
	0.852	0.73	0.756	0.503	0.617	0.648	0.76	0.789	0.748	0.698	0.788	0.846	570
	8858	7307	8791	6826	9041	7796	7310	7314	7613	6870	8750	7351	540,590
F	0.685	0.778	0.754	0.619	0.662	0.77	0.842	0.816	0.853	0.87	0.829	0.841	600
	0.623	0.676	0.67	0.614	0.642	0.681	0.818	0.765	0.799	0.755	0.752	0.751	570
	6259	5076	6655	8625	8374	6525	9599	7917	7830	4641	7349	6621	540,590
G	0.686	0.71	0.755	0.629	0.648	0.642	0.754	0.794	0.816	0.787	0.82	0.825	600
	0.678	0.68	0.731	0.6	0.661	0.627	0.742	0.77	0.808	0.769	0.81	0.771	570
	9118	8923	9553	7839	10505	8959	10177	9668	10232	10298	10021	8434	540,590
H	0.766	0.868	0.927	0.767	0.718	0.782	0.82	0.806	0.772	0.812	0.835	0.86	600
	0.758	0.852	0.974	0.81	0.676	0.76	0.787	0.753	0.709	0.811	0.786	0.759	570
	8943	9361	11270	8845	7696	7436	9169	8314	7904	10104	7892	5622	540,590

Table 28. Resazurin values measuread after 60 min of incubation at two different wavelengths for absorption (570 nm and 600 nm) and fluorescence (excitation at 540 nm and emission at 590 nm). Measurements were taken after 24 h adhesion, 48 h of biofilm formation, and 4 h of enzyme treatment. The enzyme locations, in decrea ing concentrations from top to bottom, are as follows: Protease V (A1:H3), Protease VI (A4:H6), Protease VII (A7:H9), and a positive control/blank (A10:H12).

Plate 5	1	2	3	4	5	6	7	8	9	10	11	12	
A	0.437	0.454	0.465	0.1	0.16	0.113	0.371	0.417	0.424	0.312	0.258	0.247	600
	0.553	0.545	0.574	0.163	0.261	0.198	0.475	0.531	0.529	0.431	0.364	0.36	570
	5806	5416	5146	1479	880	1182	4294	2897	3893	994	841	796	540,590
B	0.373	0.32	0.372	0.119	0.155	0.155	0.402	0.509	0.322	0.286	0.208	0.216	600
	0.478	0.421	0.477	0.18	0.189	0.2	0.503	0.626	0.426	0.378	0.313	0.296	570
	1590	2823	2653	1473	1432	1497	3880	2375	2782	2536	1412	2082	540,590
C	0.237	0.341	0.249	0.13	0.119	0.123	0.308	0.372	0.333	0.249	0.213	0.281	600
	0.333	0.441	0.348	0.167	0.174	0.185	0.405	0.484	0.425	0.35	0.307	0.382	570
	1614	2728	1937	1231	1192	1675	4012	6422	3253	2020	2328	2174	540,590
D	0.243	0.28	0.287	0.111	0.139	0.151	0.362	0.321	0.296	0.204	0.263	0.47	600
	0.336	0.388	0.398	0.178	0.22	0.242	0.463	0.422	0.402	0.307	0.358	0.578	570
	1588	1784	1654	1137	1453	1462	3344	2374	2425	1339	3591	1388	540,590
E	0.357	0.199	0.219	0.146	0.186	0.161	0.272	0.299	0.265	0.225	0.275	0.33	600
	0.468	0.309	0.317	0.22	0.259	0.26	0.371	0.398	0.36	0.318	0.366	0.438	570
	1259	1232	2348	1057	1352	1674	2631	2706	2036	2072	3494	2032	540,590
F	0.139	0.176	0.172	0.169	0.177	0.183	0.266	0.234	0.27	0.282	0.246	0.235	600
	0.24	0.292	0.28	0.262	0.275	0.288	0.36	0.334	0.367	0.388	0.342	0.338	570
	811	750	1248	1336	1399	1291	2475	2162	2248	1352	2458	1862	540,590
G	0.204	0.172	0.202	0.167	0.203	0.178	0.234	0.257	0.266	0.225	0.267	0.236	600
	0.296	0.266	0.295	0.257	0.285	0.266	0.315	0.359	0.364	0.349	0.354	0.336	570
	1049	1238	1525	1437	1630	1472	2343	2037	2457	2224	2720	2186	540,590
H	0.274	0.307	0.417	0.372	0.229	0.347	0.243	0.227	0.197	0.283	0.243	0.273	600
	0.363	0.404	0.517	0.458	0.334	0.447	0.338	0.323	0.289	0.381	0.336	0.375	570
	992	1297	1657	1203	1310	1253	2618	2771	1777	1834	1708	1465	540,590

Table 29. CV absorbance values for *C. acnes* after 4 h adhesion, 44 h biofilm formation, and 4 h treatment with enzymes. Measurements were made at wavelength 590 nm. The enzyme locations are as follows in decreasing concentrations from top to bottom: Protease V (A1:H3), Protease VI (A4:H6), Protease VII (A7:H9), and a positive control/blank (A10:H12).

Plate 6	1	2	3	4	5	6	7	8	9	10	11	12	
A	0.201	0.208	0.157	0.089	0.085	0.087	0.411	0.393	0.338	1.082	0.349	0.2	590
B	0.171	0.167	0.143	0.123	0.212	0.164	0.211	0.155	0.228	0.956	1.256	0.779	590
C	0.174	0.131	0.132	0.199	0.279	0.282	0.15	0.192	0.227	0.856	1.217	0.984	590
D	0.403	0.176	0.289	0.254	0.224	0.263	0.633	0.192	0.247	1.365	0.875	0.742	590
E	0.78	0.694	0.254	0.29	0.47	0.226	0.616	0.687	1.097	1.319	1.488	1.522	590
F	1.053	0.465	0.444	0.261	0.291	0.273	1.182	1.314	0.666	1.257	1.216	1.294	590
G	1.221	0.368	1.04	0.281	0.308	0.307	0.848	0.645	1.058	0.93	0.873	1.201	590
H	1.067	1.335	1.488	0.292	0.621	0.303	1.524	1.252	1.331	1.257	1.474	1.173	590

Table 30. Resazurin values measuread after 20 min of incubation at two different wavelengths for absorption (570 nm and 600 nm) and fluorescence (excitation at 540 nm and emission at 590 nm). Measurements were taken after 24 h adhesion, 48 h of biofilm formation, and 4 h of enzyme treatment. Control plate where rows A-B are negative control, rows C-D positive control, rows E-F buffer control and rows G-H antimicrobial control.

Plate 7	1	2	3	4	5	6	7	8	9	10	11	12	
	0.765	0.807	0.779	0.797	0.767	0.798	0.801	0.802	0.787	0.805	0.831	0.822	600
A	0.589	0.607	0.625	0.6	0.598	0.605	0.603	0.605	0.596	0.612	0.64	0.631	570
	2797	2382	3450	2458	2815	2450	2405	2392	2336	2804	2712	2593	540,590
	0.788	0.868	0.796	0.742	0.827	0.829	0.817	0.785	0.765	0.806	0.8	0.82	600
B	0.605	0.648	0.617	0.63	0.652	0.627	0.617	0.616	0.624	0.631	0.63	0.643	570
	3103	2605	2880	4407	3144	2438	2387	3042	3425	2997	2952	3049	540,590
	0.531	0.706	0.736	0.752	0.816	0.794	0.887	0.907	0.915	0.907	0.878	0.901	600
C	0.553	0.631	0.695	0.631	0.725	0.73	0.773	0.823	0.826	0.791	0.811	0.862	570
	7860	5630	8383	4552	5896	6410	5922	6801	6030	5265	7463	8982	540,590
	0.662	0.509	0.584	0.642	0.694	0.772	0.902	0.88	0.887	0.99	0.855	0.908	600
D	0.568	0.522	0.575	0.596	0.662	0.756	0.838	0.828	0.827	0.938	0.783	0.845	570
	4514	5589	6372	6253	7952	10440	7352	7831	7836	7063	7846	7711	540,590
	0.68	0.832	0.793	0.841	0.848	0.833	0.875	0.84	0.846	0.894	0.891	0.976	600
E	0.632	0.743	0.655	0.742	0.79	0.751	0.829	0.791	0.784	0.883	0.851	0.911	570
	7632	5305	3832	5337	8328	7083	7723	7225	8121	9931	8784	8112	540,590
	0.558	0.807	0.805	0.913	0.864	0.93	0.838	0.882	0.973	0.942	0.815	0.914	600
F	0.482	0.685	0.714	0.884	0.779	0.818	0.799	0.753	0.911	0.862	0.791	0.847	570
	3996	4379	6256	8653	6414	5560	8571	4333	7392	6739	9071	7793	540,590
	0.624	0.799	0.808	0.755	0.768	0.843	0.852	0.899	0.909	0.859	0.916	0.973	600
G	0.571	0.644	0.629	0.696	0.695	0.762	0.738	0.841	0.847	0.771	0.805	0.869	570
	5767	3283	3092	6640	6923	6596	5186	7298	7083	6068	5018	5325	540,590
	0.686	0.832	0.911	0.747	0.903	0.83	0.841	0.892	0.935	0.946	0.938	0.94	600
H	0.711	0.784	0.838	0.695	0.887	0.806	0.812	0.825	0.873	0.885	0.918	0.838	570
	8116	8256	6806	7449	8498	8795	9358	6798	7087	6758	9114	5273	540,590

Table 31. Resazurin values measuread after 60 min of incubation at two different wavelengths for absorption (570 nm and 600 nm) and fluorescence (excitation at 540 nm and emission at 590 nm). Measurements were taken after 24 h adhesion, 48 h of biofilm formation, and 4 h of enzyme treatment. Control plate where rows A-B are negative control, rows C-D positive control, rows E-F buffer control and rows G-H antimicrobial control.

Plate 7	1	2	3	4	5	6	7	8	9	10	11	12	
	0.109	0.111	0.116	0.112	0.126	0.12	0.117	0.121	0.123	0.132	0.132	0.138	600
A	0.239	0.256	0.239	0.251	0.26	0.258	0.255	0.257	0.257	0.263	0.268	0.272	570
	246	155	417	170	269	191	179	185	188	326	289	289	540,590
	0.115	0.12	0.127	0.138	0.163	0.131	0.13	0.144	0.169	0.154	0.16	0.153	600
B	0.247	0.269	0.264	0.256	0.299	0.271	0.268	0.277	0.303	0.277	0.293	0.278	570
	281	180	291	473	381	181	205	335	452	516	373	434	540,590
	0.135	0.125	0.16	0.134	0.161	0.192	0.245	0.232	0.226	0.224	0.216	0.277	600
C	0.222	0.196	0.228	0.249	0.28	0.284	0.364	0.338	0.341	0.345	0.329	0.375	570
	307	614	602	533	688	772	1123	1451	857	865	1616	1239	540,590
	0.12	0.151	0.139	0.136	0.18	0.204	0.214	0.214	0.261	0.311	0.242	0.337	600
D	0.205	0.194	0.242	0.22	0.266	0.283	0.308	0.306	0.367	0.42	0.34	0.467	570
	404	442	493	733	950	951	836	900	1045	1431	1567	1265	540,590
	0.139	0.179	0.144	0.191	0.196	0.176	0.208	0.178	0.245	0.276	0.239	0.306	600
E	0.234	0.281	0.273	0.314	0.311	0.277	0.319	0.276	0.338	0.393	0.337	0.421	570
	426	595	434	690	1137	1122	882	1084	906	1181	1258	1134	540,590

F	0.103	0.145	0.152	0.279	0.189	0.23	0.188	0.196	0.275	0.232	0.227	0.234	600
	0.194	0.269	0.261	0.384	0.294	0.353	0.282	0.323	0.379	0.349	0.371	0.338	570
	273	477	793	833	710	803	992	557	1163	1069	1003	1124	540,590
G	0.129	0.132	0.129	0.184	0.158	0.179	0.169	0.332	0.311	0.255	0.21	0.277	600
	0.214	0.263	0.261	0.282	0.259	0.285	0.288	0.439	0.422	0.367	0.33	0.389	570
	407	280	307	1015	896	807	622	1292	1400	962	673	1193	540,590
H	0.283	0.178	0.298	0.154	0.272	0.174	0.212	0.293	0.337	0.329	0.262	0.208	600
	0.356	0.27	0.406	0.241	0.376	0.262	0.299	0.403	0.444	0.435	0.343	0.324	570
	358	929	1062	795	1045	1204	960	875	905	992	1250	650	540,590

Table 32. CV absorbance values for *C. acnes* after 4 h adhesion, 44 h biofilm formation, and 4 h treatment with enzymes. Measurements were made at wavelength 590 nm. The enzyme locations are as follows in decreasing concentrations from top to bottom: Control plate where rows A-B are negative control, rows C-D positive control, rows E-F buffer control and rows G-H antimicrobial control.

Plate 8	1	2	3	4	5	6	7	8	9	10	11	12	
A	0.07	0.058	0.055	0.062	0.08	0.058	0.062	0.062	0.059	0.059	0.088	0.091	590
B	0.067	0.062	0.057	0.057	0.064	0.063	0.06	0.06	0.061	0.062	0.094	0.083	590
C	0.107	0.186	0.451	0.142	0.212	0.328	0.112	0.233	0.244	0.24	0.277	0.409	590
D	0.118	0.11	0.104	0.115	0.118	0.104	0.28	0.113	0.108	0.2	0.278	0.177	590
E	0.097	0.123	0.132	0.119	0.12	0.129	0.104	0.111	0.113	0.153	0.226	0.157	590
F	0.115	0.102	0.099	0.093	0.139	0.111	0.114	0.116	0.126	0.149	0.132	0.138	590
G	0.117	0.115	0.111	0.141	0.128	0.118	0.119	0.125	0.148	0.15	0.374	0.105	590
H	0.109	0.171	0.199	0.264	0.216	0.128	0.141	0.106	0.129	0.158	0.267	0.137	590

C. acnes Experiment 4

The OD_{600nm} after 24 h of cell cultivation was 1.05. This was diluted to an OD_{600nm} of 0.315 before inoculation.

Table 33. Control plate for *C. acnes* after 21 h adhesion, 45 h biofilm formation, and 4 h enzyme treatment. CV absorbance values in all columns, where rows A-B are negative control, rows C-D positive control, rows E-F buffer control and rows G-H antimicrobial control.

Plate 1	1	2	3	4	5	6	7	8	9	10	11	12
A	0.08	0.074	0.076	0.082	0.075	0.115	0.078	0.117	0.072	0.068	0.068	0.077
B	0.08	0.081	0.075	0.077	0.08	0.071	0.093	0.077	0.082	0.07	0.072	0.089
C	0.774	0.511	1.144	0.593	1.09	0.301	0.833	0.881	0.241	0.159	0.379	0.314
D	0.594	0.361	0.829	1.04	1.159	0.72	0.33	0.326	0.115	0.164	0.35	0.176
E	1.382	0.955	0.842	0.687	0.779	0.339	0.371	0.441	0.169	0.236	0.345	0.223
F	1.029	1.11	0.923	0.967	1.284	1.148	0.617	0.326	0.202	0.246	0.501	0.247
G	0.944	0.805	1.796	0.937	1.051	0.621	0.896	0.504	0.376	0.489	0.829	1.127
H	1.355	1.261	0.801	1.387	1.077	0.651	1.223	1.1	0.469	1.659	1.21	1.235

Figure 6. Image of a 96-well plate (Plate 1) after washing test plate where C1-C2 has been washed one time with saline, and D1-D2 washed one time with DPBS.

Table 34. CV absorbance values for *C. acnes* after 21 h adhesion, 45 h biofilm formation, and 4 h treatment with enzymes. The enzyme locations, in decreasing concentrations from top to bottom, are as follows: Nuclease I (A1:H3), Nuclease II (A4:H6), Lysozyme I (A7:H9), Unknown proteins (A10:H11) and a positive control/blank (A12:H12).

Plate 2	1	2	3	4	5	6	7	8	9	10	11	12
A	0.434	0.197	0.426	0.63	0.484	0.611	1.027	1.203	1.164	1.869	2.48	2.116
B	0.497	0.449	0.591	0.394	0.248	0.719	0.789	1.193	0.754	0.767	2.284	2.374
C	0.486	0.613	0.64	0.485	0.235	0.392	0.509	0.756	1.106	1.063	1.427	1.813
D	0.462	0.32	0.591	0.584	0.404	0.269	0.203	0.233	0.292	0.651	0.537	2.319
E	0.474	0.436	0.548	0.471	0.496	0.291	0.184	0.312	0.351	1.576	2.665	2.802
F	0.553	0.523	0.658	0.498	0.27	0.467	0.262	0.222	0.527	0.94	2.451	2.418
G	0.656	0.87	0.547	0.487	0.406	0.364	0.381	0.279	0.318	0.523	1.211	2.451
H	0.503	0.335	0.45	0.579	0.338	0.373	0.321	0.369	0.516	1.289	0.684	2.318

Figure 7. Image of a 96-well plate (Plate 2) after CV staining, showing biofilm after 4 h enzyme treatment, and 20 min of incubation with CV. The enzyme concentrations decrease from top to bottom, and the wells are organized as follows: Nuclease I (A1:H3), Nuclease II (A4:H6), Lysozyme I (A7:H9), Unknown proteins (A10:H11) and a positive control/blank (A12:H12).

Table 35. CV absorbance values for *C. acnes* after 21 h adhesion, 45 h biofilm formation, and 4 h treatment with enzymes. The enzyme locations, in decreasing concentrations from top to bottom, are as follows: Protease IV (A1:H3), Protease III (A4:H6), Protease II (A7:H9), Unknown proteins (A10:H11) and a positive control/blank (A12:H12).

Plate 3	1	2	3	4	5	6	7	8	9	10	11	12
A	0.347	0.38	0.294	0.331	0.441	0.399	0.702	0.746	0.563	1.764	1.86	2.198
B	0.38	0.453	0.34	0.305	0.286	0.202	0.291	0.297	1.09	2.191	2.009	1.356
C	0.423	0.56	0.577	0.346	0.318	0.264	0.299	1.172	1.329	2.289	3.624	2.192
D	0.338	0.363	0.497	0.22	0.255	0.313	0.18	1.205	1.226	2.134	2.29	1.963
E	0.575	0.432	0.417	0.383	0.432	0.326	0.398	1.467	1.455	1.766	2.214	1.491
F	0.69	0.559	0.805	0.634	0.341	0.364	1.379	1.596	2.259	2.59	1.392	2.069
G	0.331	0.532	0.463	0.417	0.405	0.21	0.329	0.495	1.061	1.419	2	2.863
H	0.609	0.432	0.455	0.51	0.531	0.59	1.684	1.621	2.4	1.718	2.505	2.085

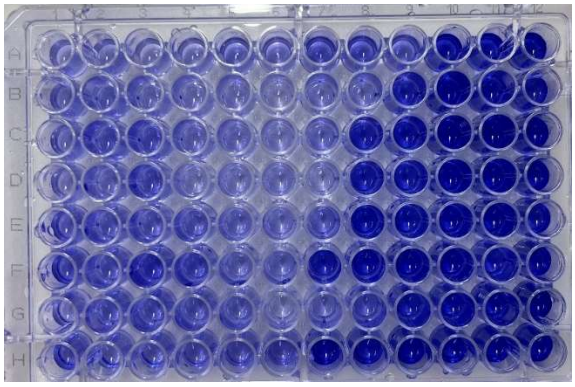

Figure 8. Image of a 96-well plate (Plate 3) after CV staining, showing biofilm after 4 h enzyme treatment, and 20 min of incubation with CV. The enzyme concentrations decrease from top to bottom, and the wells are organized as follows: Protease IV (A1:H3), Protease III (A4:H6), Protease II (A7:H9), Unknown proteins (A10:H11) and a positive control/blank (A12:H12).

Table 36. CV absorbance values for *C. acnes* after 21 h adhesion, 45 h biofilm formation, and 4 h treatment with enzymes. The enzyme locations, in decreasing concentrations from top to bottom, are as follows: Protease V (A1:H3), Protease VI (A4:H6), Protease VII (A7:H9), Unknown proteins (A10:H11) and a positive control/blank (A12:H12).

Plate 4	1	2	3	4	5	6	7	8	9	10	11	12
A	4.0+	4.0+	4.0+	0.349	0.65	0.536	4.0+	4.0+	4.0+	1.071	1.395	1.154
B	4.0+	4.0+	4.0+	1.158	0.695	0.486	3.768	2.947	2.966	1.071	1.275	1.309
C	2.199	2.741	2.413	0.985	0.989	0.573	1.796	3.336	3.522	1.823	1.938	1.411
D	1.913	1.482	0.633	0.429	0.903	0.82	3.18	2.772	2.676	2.563	1.597	1.645
E	0.922	0.626	0.56	0.355	1.305	1.439	0.335	2.132	1.9	2.138	2.132	2.127
F	0.948	0.395	0.398	0.264	0.333	0.298	1.343	1.317	2.692	2.842	2.352	2.38
G	0.525	0.407	0.337	0.288	0.375	0.224	1.51	0.925	2.14	2.462	2.515	2.775
H	0.341	0.32	0.351	0.37	0.596	0.442	1.52	1.334	1.066	1.21	1.435	1.658

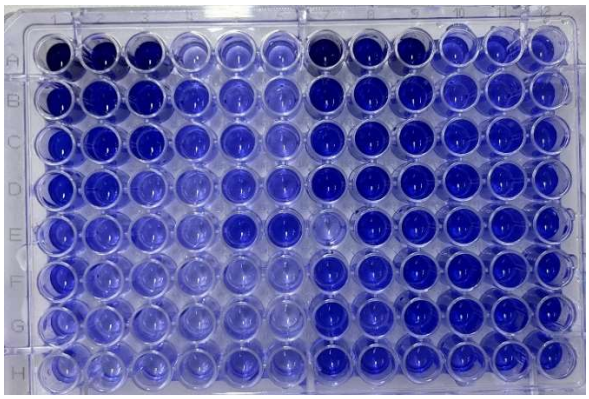

Figure 9. Image of a 96-well plate (Plate 4) after CV staining, showing biofilm after 4 h enzyme treatment, and 20 min of incubation with CV. The enzyme concentrations decrease from top to bottom, and the wells are organized as follows: Protease V (A1:H3), Protease VI (A4:H6), Protease VII (A7:H9), Unknown proteins (A10:H11) and a positive control/blank (A12:H12).

C. acnes Experiment 5

The OD_{600nm} after 24 h of cell cultivation was 1.4. This was diluted to an OD_{600nm} of 0.2 before inoculation.

Table 37. CV absorbance values for *C. acnes* after 21 h adhesion, 45 h biofilm formation, and 4 h treatment with enzymes. The enzyme locations, in decreasing concentrations from top to bottom, are as follows: Nuclease I (A1:H3), Nuclease II (A4:H6), Lysozyme I (A7:H9), positive control (A10:H11) and a negative control (A12:H12).

Plate 2	1	2	3	4	5	6	7	8	9	10	11	12
A	1.3	0.661	0.77	1.111	1.654	1.646	4,0+	4,0+	4,0+	4,0+	4,0+	0.869
B	0.486	0.389	0.415	0.348	0.331	0.355	4,0+	4,0+	4,0+	4,0+	4,0+	0.679
C	0.553	0.267	0.357	0.487	0.501	0.473	2.821	4,0+	3.84	4,0+	4,0+	0.665
D	0.345	0.416	0.399	0.371	0.501	0.351	3.247	3.737	4,0+	4,0+	4,0+	0.426
E	0.26	0.423	0.385	0.36	0.331	0.356	1.174	0.921	4,0+	4,0+	4,0+	0.278
F	0.351	0.403	0.344	0.413	0.424	0.363	1.565	0.397	2.598	4,0+	4,0+	0.332
G	0.55	0.435	0.405	0.309	0.408	0.351	0.576	0.564	3.303	4,0+	4,0+	0.577
H	0.495	0.625	0.362	0.48	0.373	0.391	0.374	0.861	3.771	4,0+	4,0+	1.179

Table 38. CV absorbance values for *C. acnes* after 21 h adhesion, 45 h biofilm formation, and 4 h treatment with enzymes. The enzyme locations, in decreasing concentrations from top to bottom, are as follows: Protease IV (A1:H3), Protease III (A4:H6), Protease II (A7:H9), positive control (A10:H11) and a buffer control (A12:H12).

Plate 3	1	2	3	4	5	6	7	8	9	10	11	12
A	1,003	0,773	0,881	1,645	1,447	1,679	0.947	1.453	0.668	4,0+	4,0+	4,0+
B	0,906	1,03	0,48	0,959	0,931	0,606	1.038	2.217	1.698	4,0+	4,0+	4,0+
C	1,205	0,989	0,749	0,525	0,861	0,545	1.548	2.008	1.394	4,0+	4,0+	4,0+
D	1,048	1,373	0,763	0,913	0,934	1,242	1.569	2.131	1.559	4,0+	4,0+	4,0+
E	1,225	0,762	0,772	0,824	1,173	1,415	1.628	1.894	1.647	4,0+	4,0+	3,798
F	1,776	1,767	1,806	0,61	0,818	1,18	2.604	3.867	2.603	4,0+	4,0+	4,0+
G	2,258	2,15	1,61	0,813	1,038	1,231	2.841	4,0+	3.612	4,0+	4,0+	4,0+
H	3,503	3,431	3,461	1,456	0,927	1,292	2.882	4,0+	3.175	4,0+	4,0+	4,0+

Table 39. CV absorbance values for *C. acnes* after 21 h adhesion, 45 h biofilm formation, and 4 h treatment with enzymes. The enzyme locations, in decreasing concentrations from top to bottom, are as follows: Protease V (A1:H3), Protease VI (A4:H6), Protease VII (A7:H9), positive control (A10:H11) and an antimicrobial control (A12:H12).

Plate 4	1	2	3	4	5	6	7	8	9	10	11	12
A	4,0+	4,0+	4,0+	3.127	0.528	4,0+	4,0+	4,0+	4,0+	4,0+	4,0+	3,88
B	4,0+	4,0+	4,0+	3.355	4,0+	4,0+	4,0+	4,0+	4,0+	4,0+	4,0+	4,0+
C	4,0+	4,0+	4,0+	2.892	3.994	4,0+	4,0+	4,0+	4,0+	4,0+	4,0+	4,0+
D	4,0+	4,0+	4,0+	4,0+	4,0+	4,0+	4,0+	4,0+	4,0+	4,0+	4,0+	4,0+
E	4,0+	4,0+	4,0+	4,0+	4,0+	4,0+	4,0+	4,0+	4,0+	4,0+	4,0+	4,0+
F	4,0+	4,0+	4,0+	4,0+	4,0+	4,0+	4,0+	3.452	4,0+	4,0+	4,0+	4,0+
G	4,0+	4,0+	3,764	4,0+	4,0+	4,0+	4,0+	3.576	3.977	4,0+	4,0+	4,0+
H	4,0+	4,0+	4,0+	4,0+	4,0+	4,0+	4,0+	4,0+	4,0+	4,0+	4,0+	4,0+

Appendix C

Detailed information on chemical solutions

Tris/$CaCl_2$-buffer

TRIS

$CaCl_2$ x $2H_2O$

Deionized water

HCl (37%)

Glycerol dilution buffer

Glycerol

Deionized water

Tris/$CaCl_2$-buffer

Brain Heart Infusion (BHI) Broth

Beef heart

Disodium hydrogen phosphate

Peptone

Calf brains

Sodium chloride

D(+)-glucose

Phosphate Buffered Saline (PBS)

Sodium chloride

Potassium chloride

Sodium phosphate dibasic

Pottasium phosphate monobasic

Distilled water

Dulbecco's Phosphate Buffered Saline (D-PBS)

Calcium chloride

Potassium chloride

Magnesium chloride hexahydrate

Sodium chloride

Sodium phosphate dibasic

Distilled water

Appendix D

Product information document

(This is a proposed product not yet available on the market).

ClearZyme

Purifying Face Gel 30ml

CLEARZYME

For a healthy skin microbiome

The Purifying Face Gel has been specifically developed for acne-prone skin to clear blemishes and help prevent new acne outbreaks, all while maintaining the natural microbiome of your skin.

Key ingredients include biomimetic peptide, endonuclease, niacinamide, glycerin, and xylitol. The biomimetic peptide protects the skin's microbiome by inhibiting the growth of *Cutibacterium acnes* and breaking down its biofilm to prevent inflammatory skin damage, promoting healthier skin. Endonuclease non-selectively degrades all forms of DNA and RNA, disrupting the biofilm matrix of *Cutibacterium acnes*. Niacinamide reduces sebum production, preventing the formation of acne lesions. Glycerin acts as a humectant, supporting the skin's barrier function. Xylitol, a naturally occurring polyol, also acts as a humectant and balances the skin's microbiome. ClearZyme Purifying Face Gel features a lightweight gel texture that is quickly and effortlessly absorbed by the skin. It is free from alcohol, fragrance, and preservatives, making it suitable for sensitive skin.

Ingredients

Aqua, glycerin, caprylic/capric triglyceride, xylitol, niacinamide, polyglyceryl-3 cocoate, hydrogenated lecithin, lecithin, pentylene glycol, palmitoyl pentapeptide-4, tromethamine, xanthan, nuclease, magnesium chloride.

How to use

By itself: Dispense 1-2 pumps onto your fingertips and gently massage into your face every night after cleansing.

In combination with exfoliating serum: For enhanced anti-acne effects, we recommend using ClearZyme Purifying Face Gel in combination with ClearZyme Exfoliating Serum (*proposed product*) containing a protease enzyme. Apply the serum at night after cleansing, and the Purifying Face Gel after cleansing in the morning.